Check for updates

European Journal of Organic Chemistry

EurJOC
European Journal of Organic Chemistry

Chemistry Europe
European Chemical Societies Publishing

REVIEW OPEN ACCESS

π-Extended Silyl Enolates as Emerging Platforms in Radical Chemistry

Debora Guazzetti | Kelly Bugatti | Claudio Curti | Franca Zanardi

Department of Food and Drug, University of Parma, Parma, Italy

Correspondence: Claudio Curti (claudio.curti@unipr.it) | Franca Zanardi (franca.zanardi@unipr.it)

Received: 12 June 2026 | **Revised:** 12 June 2026 | **Accepted:** 20 July 2026

Keywords: π-extended silyl enolates | photoredox catalysis | principle of vinylogy | radicals | umpolung

ABSTRACT

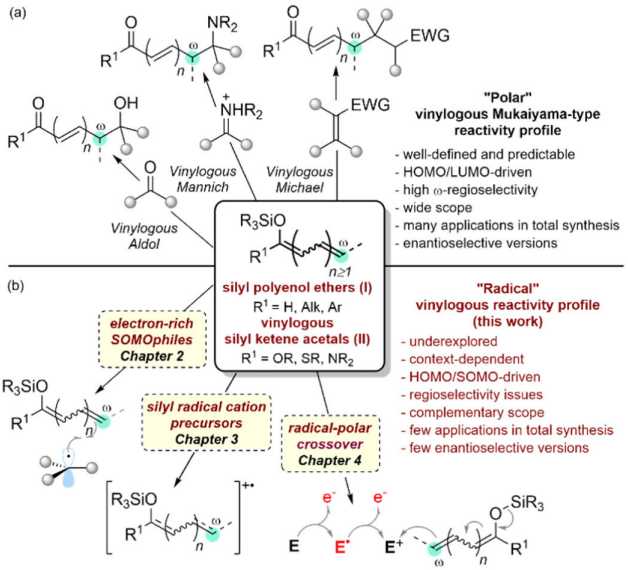
π-Extended silyl polyenol ethers and their related silyl ketene acetals are well-established vinylogous nucleophiles in polar transformations; however, their potential in radical chemistry has only recently emerged. Owing to their intrinsically electron-rich character, arising from conjugated π-systems and σ-donating silyl groups, these substrates display unique reactivity under single-electron transfer conditions. This review provides a comprehensive overview of their behavior in radical-mediated processes, highlighting their versatile role as electron-rich SOMOphiles, radical precursors, and nucleophilic partners in radical–polar crossover manifolds. A key concept underlying their reactivity is the umpolung induced by single-electron oxidation, which converts nucleophilic vinylogous enolates into electrophilic radical cation or keto-allyl radical intermediates, thereby unlocking unconventional bond-forming pathways inaccessible through traditional two-electron chemistry. Moreover, these systems exhibit a distinctive propensity for remote functionalization at γ-, ε-, and η-positions, governed by electronic delocalization and radical stabilization across the extended π-framework. Recent advances in photoredox catalysis, electrochemistry, and transition metal-mediated methodologies have significantly expanded the scope and synthetic utility of these transformations, enabling efficient C—C and C—heteroatom bond formation, enantioselective variants, and applications in the synthesis of complex molecules. Collectively, these developments position π-extended silyl polyenol ethers as versatile and tunable platforms in modern radical chemistry.

1 | Introduction

Silyl polyenol ethers (**I**, Scheme 1) and their (thio)ester- or amide-derived silyl ketene acetal congeners (**II**) rank among the most extensively studied and widely employed preformed, vinylogous nucleophiles in organic synthesis [1]. In both their linear format and cyclic format, within the manifold of "polar" ionic reactivity, they have served as preformed extended enolates, providing a paradigmatic illustration of the principle of vinylogy [2], whereby the electronic effects and reactivity of a specific functional group within a conjugated π-system are transmitted through the chain up to the most distant ω-position. In this context, polyenolates **I** and **II** have enabled highly efficient carbon–carbon bond formation through Mukaiyama-type reactions and related processes—e.g., vinylogous Mukaiyama aldol [3], Mannich [4], and Michael [5] addition reactions—giving access to a plethora of highly functionalized, chiral chemotypes (Scheme 1a). The success of **I** and **II** in polar chemistry stems from their well-defined electronic distribution and the ability to finely tune their behavior through substitution patterns along the π-extended chain and the nature of the silyl group. This enables predictable regioselectivity, primarily favoring reactivity at the most remote position of the polyene chain (Further supporting the key role of silicon in promoting reactivity at the most remote site of the polyenolate chain, other metal polyenolates preferentially undergo electrophilic attack at the α-position. For a recent account on α-selective alkylation of polyenoic acids by the use of chiral lithium amides, see: ref. [6]). As a result, their polar reactivity has been thoroughly investigated and exploited in both methodological and target-oriented syntheses, giving rise to a plethora of catalytic, regio-, diastereo-,

This is an open access article under the terms of the Creative Commons Attribution License, which permits use, distribution and reproduction in any medium, provided the original work is properly cited.

© 2026 The Author(s). *European Journal of Organic Chemistry* published by Wiley-VCH GmbH.



SCHEME 1 | Silyl (poly)enol ethers (**I**) and π-extended silyl ketene acetals (**II**) as privileged scaffolds in: (a) "polar" vinylogous Mukaiyama-type transformations versus (b) radical-mediated vinylogous transformations (this work).

and enantioselective versions. In contrast, the radical chemistry of polyenes **I** and **II** has remained comparatively underexplored for many years, despite the conceptual appeal of engaging these conjugated systems under open-shell conditions (For a recent review article on this topic, see: ref. [7]). While polar reactions rely on the intrinsic nucleophilicity of the dienolate framework (highest occupied molecular orbital (HOMO)-driven transformations), radical processes unlock fundamentally different reactivity pathways, governed by single-electron transfer (SET) events, radical delocalization, and polarity-matching principles distinct from classical ionic paradigms (singly occupied molecular orbital (SOMO)-driven transformations). In this setting, these scaffolds can no longer be viewed solely as vinylogous enolate congeners, but rather as versatile radical precursors or coupling partners toward open-shell intermediates capable of engaging nucleophilic or electrophilic radical species in a complementary fashion. The growing interest in radical-based synthetic strategies [8]—driven by advances in photoredox catalysis [9], electrochemistry [10], and radical relay processes [11]—has recently prompted a reassessment of silyl polyenol ethers and the corresponding silyl ketene acetals as valuable partners in radical transformations. Notably, their conjugated π-systems and silicon substituents impart unique stabilization and reactivity features to the corresponding allyl radical intermediates, enabling site-selective functionalization patterns or umpolung reactivities that are often inaccessible under polar conditions. These developments highlight a conceptual shift on the use of **I** and **II** when passing from chemically well-defined nucleophilic species with predictable reactivity in two-electron processes, to versatile entities displaying context-dependent and multifaceted reactivity profiles in single-electron reaction manifolds.

This review aims to provide a comprehensive and critical overview of the radical reactivity of polyenes **I** and **II**. Emphasis is placed on the diverse ways in which these π-extended, silicon-stabilized systems engage in radical processes, highlighting their versatility as both radical acceptors and radical precursors. Recent advances have revealed that **I** and **II** display rich and tunable reactivity under single-electron conditions, enabling bond constructions and reactivity patterns that are not readily accessible through conventional two-electron pathways. As a result, these compounds have emerged as strategic platforms in the development of modern radical methodologies.

This review is organized into three main sections (Scheme 1b), each addressing a distinct radical-mediated reactivity manifold involving electron-rich substrates **I** and **II**. The first section examines radical addition processes in which these polyenes act as electron-rich SOMOphiles, undergoing direct coupling with carbon- or heteroatom-centered electrophilic radicals across the conjugated enol ether framework. Emphasis is placed on the factors controlling reactivity and selectivity, as well as on the synthetic value of these transformations. The second section examines silyl polyenol ethers as radical precursors, concentrating on transformations initiated by (photo)chemical single-electron oxidation of **I** and **II** to generate the corresponding silyl radical cations. These highly reactive and electron-poor intermediates serve as pivotal species that enable bond reorganization, fragmentation, or further radical engagement, thereby expanding the repertoire of accessible molecular architectures. The third section focuses on radical-mediated vinylogous addition reactions in which silyl polyenol ethers operate as privileged polar nucleophiles within net-neutral or net-oxidative radical–polar crossover (RPC) manifolds. In these processes, initial radical activation enables the in situ formation of highly electrophilic intermediates—such as primary benzylic carbocations or iminium ions—that are otherwise difficult to access, and which are subsequently intercepted by electron-rich silyl polyenol ethers through traditional, polar vinylogous bond-forming events.

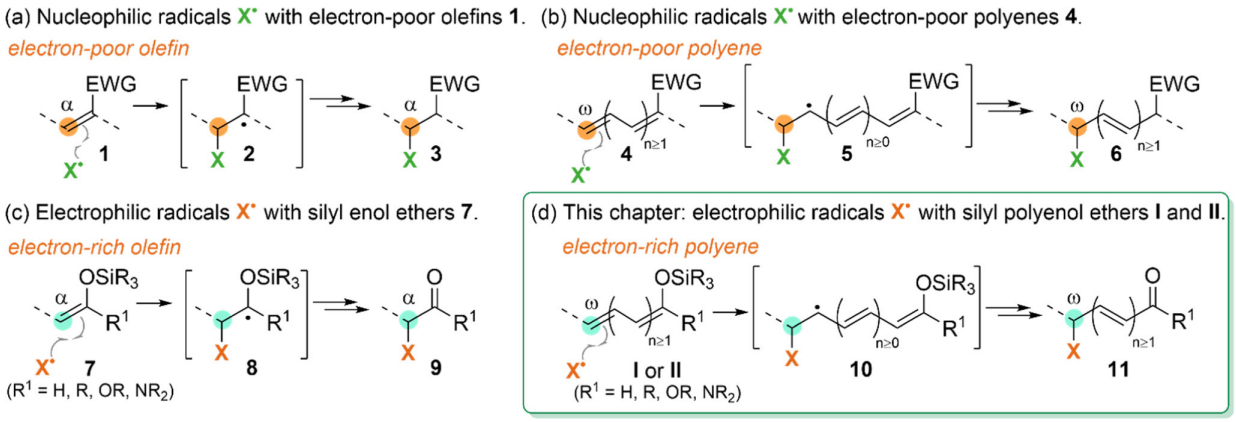
Overall, this review aims to delineate the fundamental principles and emerging trends that define the radical chemistry of silyl polyenol ethers **I** and **II**, showcasing their growing importance as privileged scaffolds in radical synthesis and setting the stage for future developments in this rapidly evolving field.

2 | Silyl Polyenol Ethers as Electron-Rich SOMOphiles

The Giese reaction—i.e., the conjugate addition of an open-shell intermediate to an electron-deficient olefin system [12]—has long served as a cornerstone in radical chemistry, providing a direct and efficient platform for unlocking unprecedented disconnections (Scheme 2a) [13].

In 2021, Welin and coworkers examined the concept of radical philicity, defined as the tendency of a given radical to react either as a nucleophile or an electrophile [14]. Supported by previous reports focusing on quantitative measurements [15], electrophilicity and nucleophilicity index [16], and theoretical calculations [17], these authors provided a comprehensive analysis of open-shell intermediates philicity, outlining how their electrophilic or nucleophilic behavior could be predicted from structural features. Hence, it was assessed that a radical species is considered nucleophilic if it has the tendency to react with electron-deficient olefins, while the open-shell intermediate is

10990690, 0, Downloaded from https://chemistry-europe.onlinelibrary.wiley.com/doi/10.1002/ejoc.70753 by Claudio Curti - University Degli Studi Di Parma Stampa Universitaria Parmense , Wiley Online Library on [31/08/2026]. See the Terms and Conditions (https://onlinelibrary.wiley.com/terms-and-conditions) on Wiley Online Library for rules of use; OA articles are governed by the applicable Creative Commons License



SCHEME 2 | General SOMOphilic reactivity of diversely substituted olefin systems coupling with radical intermediates. (a) Reaction of electron-rich open-shell species with electron-poor olefins **1**. (b) Interaction of electron-deficient polyenes **4** with nucleophilic radical partners. (c) Reaction of electron-rich silyl enol ethers **7** with electrophilic open-shell intermediates. (d) The theme of this section: electron-rich π-extended enol ethers **I** and **II** as SOMOphilic species in the presence of electrophilic radicals. EWG = electron-withdrawing group.

regarded as electrophilic if its preferred reaction partners are electron-rich alkenes. Therefore, nucleophilic radicals commonly participate in Giese-type additions to electron-deficient olefins [18]. Despite the wide diffusion of this reaction, its application to polyunsaturated electron-poor systems has been less investigated (Scheme 2b) (As a representative example of Giese-type addition of nucleophilic radicals to electron-deficient olefins, see: ref. [19]). Indeed, compounds of type **4** could conveniently react with nucleophilic radicals to provide the corresponding remotely functionalized polyene products **6**. Conversely, when considering electrophilic open-shell intermediates, preformed silyl enol ethers **7** have emerged as particularly powerful electron-rich SOMOphiles, to achieve the α-functionalized carbonyl compounds **9** (Scheme 2c) [20, 21]. While being less explored, their vinylogous π-extended counterparts [1], namely silyl polyenol ethers or silyl ketene acetals **I** and **II** (Scheme 2d), have likewise demonstrated the ability to leverage their electron density to proficiently interact with electrophilic single-electron species, providing allyl radical intermediates **10.** This unveils remote functionalization pathways that provide access to diversely substituted polyunsaturated carbonyl compounds **11**. Their reactivity has positioned them as key partners in the development of new radical methodologies for complex molecule construction, and this will be addressed in the present section. Figure 1 summarizes the radical precursors that have been used to generate the electrophilic open-shell species discussed in this section. These include thiocyanates, alkyl halides, Katritzky salts, sulfonyl chlorides, and *S*-perfluoroalkyl sulfoximines, which generate the corresponding radicals directly via SET processes. In contrast, 1,3-dicarbonyl compounds, benzoxazolyl acetates, and acetic ester derivatives form radical species via enolate formation.

In analogy with what was observed for polar, vinylogous reactions involving polyenolate-like compounds with electrophilic partners [22, 23], the interaction of π-extended silyl polyenol ether **I** or **II** (Scheme 3) with radical intermediates also raises regioselectivity issues. In principle, such processes could furnish either the corresponding deconjugated α-functionalized products (α-**11**), the vinylogous partially conjugated γ-functionalized counterparts (γ-**11**), or the fully conjugated hypervinylogous polyunsaturated carbonyl compounds (ω-**11**, or mixtures thereof, Scheme 3). Notably, it has been observed that electron-rich olefins preferentially react with electrophilic radical intermediates at the most remote site, although only a very limited number of studies have investigated the theoretical basis of this behavior.

One such study was very recently reported by Guo and coworkers, during a study on the electrochemical nickel-catalyzed vinylogous radical addition of suitable benzoxazolyl acetate radicals to silyl polyenol ethers **12a–d** (Figure 2). In that work, which will be detailed later in this section (Scheme 20), selective functionalization at the most remote η-position of the π-extended donor systems was invariably witnessed [24]. To rationalize the origin of this regioselectivity, the authors

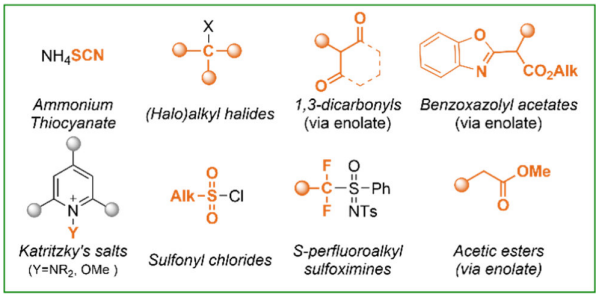
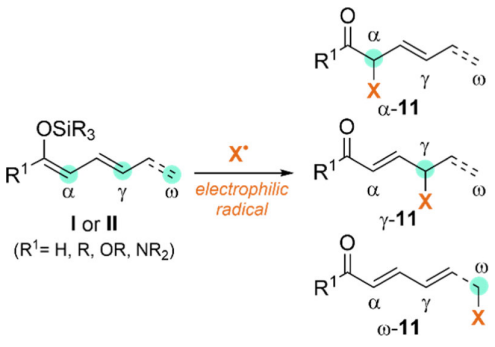


FIGURE 1 | Set of radical precursors featured in the reactions described in this section. Radical moiety precursors in orange.



SCHEME 3 | Regioselectivity issue of the reaction of open-shell intermediates **X**• with π-extended silyl polyenol ethers **I** or silyl ketene acetals **II**.

10990690, 0, Downloaded from https://chemistry-europe.onlinelibrary.wiley.com/doi/10.1002/ejoc.70753 by Claudio Curti - University Degli Studi Di Parma Stampa Universitaria Parmense , Wiley Online Library on [31/08/2026]. See the Terms and Conditions (https://onlinelibrary.wiley.com/terms-and-conditions) on Wiley Online Library for rules of use; OA articles are governed by the applicable Creative Commons License

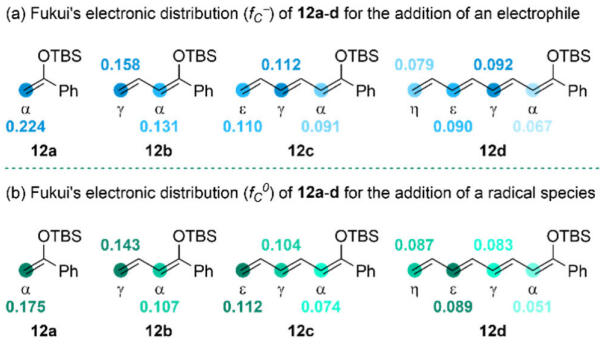


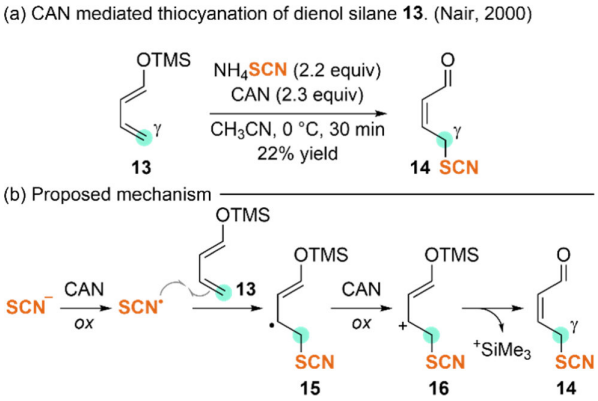
FIGURE 2 | Calculated electronic distribution in π-extended systems **12a–d**: (a) condensed Fukui's functions (f_C^-) for the additions of an electrophile; (b) condensed Fukui's functions (f_C^0) for the coupling of a radical species.

performed density functional theory (DFT) calculations on substrates **12a–d**. Condensed Fukui functions (f_C^-) for an electrophilic attack [25] (Figure 2a) revealed that, as the π-system became more extended, the ionic reactivity pattern appeared less differentiated across the different positions. This trend was supported by the values calculated for **12c** ($\alpha = 0.091$, $\gamma = 0.112$, $\varepsilon = 0.110$) and **12d** ($\alpha = 0.067$, $\gamma = 0.092$, $\varepsilon = 0.090$, $\eta = 0.079$), in contrast with the more pronounced site differentiation observed for **12a** ($\alpha = 0.224$) and **12b** ($\alpha = 0.131$, $\gamma = 0.158$).

Conversely, the condensed Fukui functions for radical attack (f_C^0) [26] (Figure 2b) indicated that, in vinylogous systems, increasing the length of the olefin chain progressively favored radical addition at the terminal position relative to two-electron processes. In fact, for molecules **12a** and **12b** the calculated values were $\alpha = 0.175$ and $\alpha = 0.107$, $\gamma = 0.143$, respectively, while in more extended systems the corresponding indices were $\alpha = 0.074$, $\gamma = 0.104$, $\varepsilon = 0.112$ for **12c** and $\alpha = 0.051$, $\gamma = 0.083$, $\varepsilon = 0.089$, $\eta = 0.087$ for **12d**. Moreover, the analysis of topographic steric maps and the percentages of buried volume revealed that steric hindrance effects rose steadily from η- to α-addition, making the former more favorable. In addition to these electronic and steric factors, a thermodynamic contribution was possibly considered. Indeed, the allylic nature of the radical intermediate generated upon radical conjugate addition to the olefin system (e.g., compound **10** in Scheme 2) could provide a further element of stabilization.

The first reported example of remote functionalization of dienolate equivalents with radical intermediates dates back to 2000, when, within a broader study, the Nair's group introduced a cerium ammonium nitrate (CAN)-mediated thiocyanation of electron-rich silyl dienol ether **13**, in the presence of ammonium thiocyanate (NH_4SCN, Scheme 4a) [27]. Using excess CAN (2.3 equiv), the reaction furnished the desired γ-functionalized product **14** in a quite poor 22% isolated yield [28].

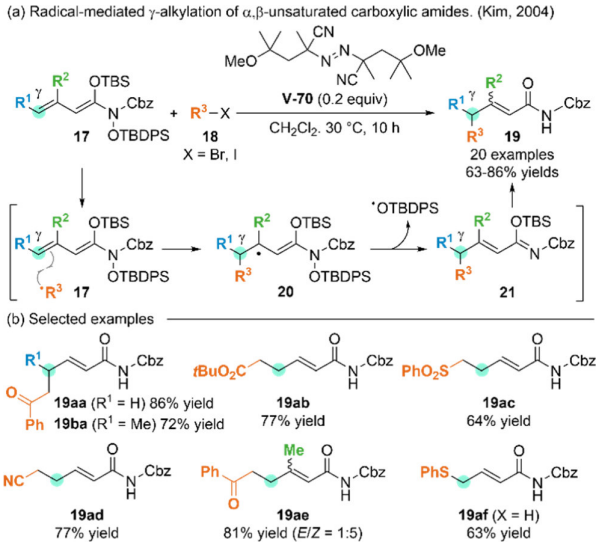
The proposed mechanism proceeded via the initial CAN-promoted oxidation of thiocyanate anion to provide the corresponding electrophilic thiocyanate radical, which could react with electron-rich SOMOphile **13** at the γ-position to obtain the open-shell intermediate **15** (Scheme 4b). Then, further oxidation performed by stoichiometric CAN provided carbocation **16**, which yielded α,β-unsaturated carbonyl compound **14**



SCHEME 4 | Seminal, radical-mediated remote thiocyanation of silyl dienol ether **13** promoted by CAN, as reported by Nair and coworkers.

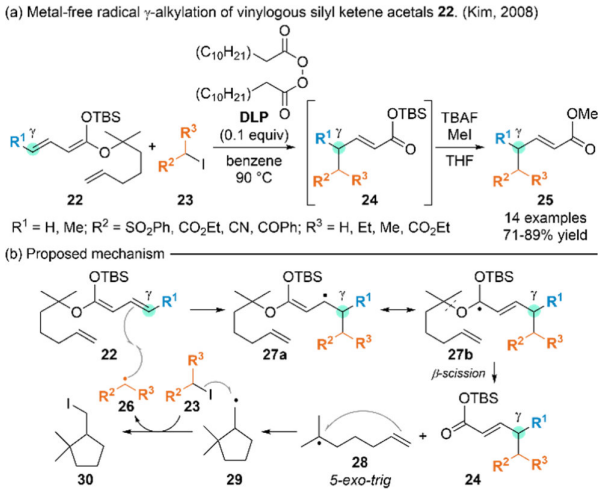
after desilylation. Later in 2004, Lim and coworkers reported the γ-functionalization of silyl ketene *N,O*-acetals **17** with a set of alkyl- or heteroatom-containing radical precursors **18** (Scheme 5a) [29]. The reaction was carried out in the presence of 2,2′-azobis(4-methoxy-2,4-dimethylvaleronitrile (**V-70**) as the radical initiator, achieving a collection of 20 different remotely functionalized α,β-unsaturated amides **19** in good yields (63%–86%) and with complete γ-regioselectivity (Scheme 5b). Based on a previous work reported by the same research group on similar yet nonvinylogous systems [30], the authors proposed that the addition step of electrophilic open-shell intermediates from **18** to electron-rich SOMOphiles **17** generated allyl radical intermediates **20** (Scheme 5a). The latter, upon N—O bond homolytic cleavage, furnished the γ-functionalized silyl enol amides **21**, which delivered the desired products **19** after aqueous workup.

In 2008, the Kim's group evaluated the reactivity of vinylogous silyl ketene acetals **22** toward a range of substituted alkyl iodides **23** under metal-free conditions, in the presence of dilauroyl peroxide (DLP) as the radical initiator (Scheme 6a) [31]. A series

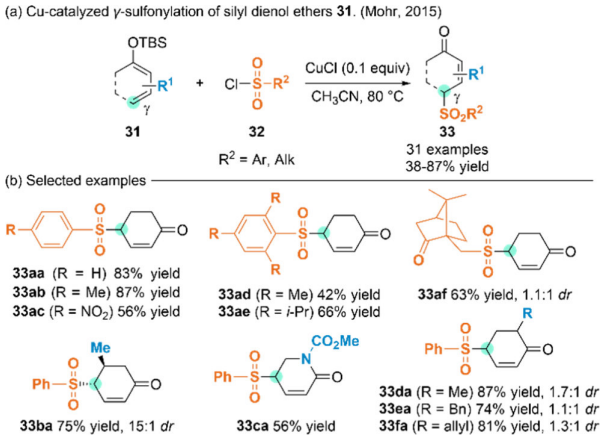


SCHEME 5 | γ-Functionalization of vinylogous silyl ketene *N,O*-acetals **17** from α,β-unsaturated amides performed by Lim and coworkers.

10990690, 0, Downloaded from https://chemistry-europe.onlinelibrary.wiley.com/doi/10.1002/ejoc.70753 by Claudio Curti - University Degli Studi Di Parma Stampa Universitaria Parmense , Wiley Online Library on [31/08/2026]. See the Terms and Conditions (https://onlinelibrary.wiley.com/terms-and-conditions) on Wiley Online Library for rules of use; OA articles are governed by the applicable Creative Commons License



SCHEME 6 | Remote radical functionalization of unsaturated silyl ketene acetals **22**. DLP = dilauroyl peroxide.

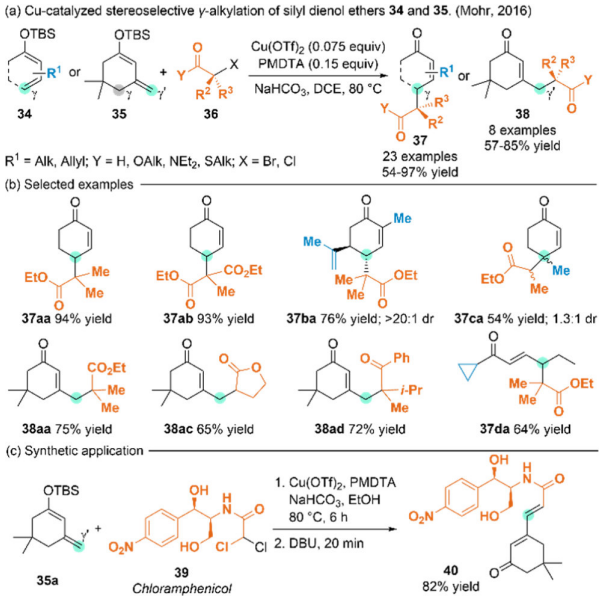


SCHEME 7 | Copper-catalyzed γ-sulfonylation of dienol silanes **31** with sulfonyl chlorides **32** developed by Mohr et al.

of remotely functionalized silylated esters **24** were obtained and readily converted into more stable methyl ester derivatives **25** by treatment with TBAF and MeI. Through this strategy, 14 γ-functionalized α,β-unsaturated methyl esters **25** were accessed in overall good yields (71%–89%) and with complete regioselectivity. According to the authors, a radical chain propagation mechanism was operative. As outlined in Scheme 6b, electrophilic radical species **26**, generated by reduction of alkyl iodides **23**, reacted with electron-rich silyl ketene acetals **22** to form open-shell intermediates **27a**/**27b**, which underwent β-scission to furnish the TBS-esters **24** together with tertiary radical **28**. The latter rapidly underwent 5-*exo*-*trig* cyclization to give the primary alkyl radical **29**, which, after halogen-atom transfer from alkyl iodides **26**, delivered by-product **30** while regenerating radical **26**, thus sustaining the chain.

After these seminal contributions, Mohr and coworkers systematically explored the reactivity of π-extended silyl enol ethers toward suitable electrophilic open-shell intermediates, focusing on copper-, manganese-, and iron-assisted radical pathways to selectively provide remotely functionalized α,β-unsaturated carbonyl compounds. The first example of a copper-catalyzed strategy enabling the selective γ-sulfonylation of silyl dienol ethers dates back to 2015 (Scheme 7a), when the reaction between electron-rich dienes **31** and variously substituted aryl- and alkyl-sulfonyl chlorides **32** was reported, in the presence of a catalytic amount of copper(I) chloride [32]. This protocol provided a collection of γ-sulfonylated α,β-unsaturated carbonyl compounds **33** in moderate-to-good yields (38%–87%), with complete regioselectivity. The method proved to be broadly applicable to aryl sulfonyl chlorides bearing either electron-donating or electron-withdrawing substituents (**33aa**–**33ae**, Scheme 7b). Aliphatic camphorsulfonyl chloride also participated smoothly, affording compound **33af** in a 63% yield, although without any induced stereoselectivity (1.1:1 *dr*). From a mechanistic point of view, the researchers proposed the formation of an electrophilic sulfonyl radical intermediate capable of efficiently engaging the electron-rich SOMOphiles **31** (not shown). To assess whether an ionic pathway could be operative, they carried out the reaction using a stoichiometric amount of CuCl and, additionally, replaced it with various Lewis acids such as TMSOTf, $AlCl_3$, $Ti(OiPr)_4$, and $ZnBr_2$, which are unlikely to participate in single-electron processes. Under these conditions, however, the sulfonylation was completely inhibited, supporting the involvement of a radical mechanism. Finally, the absence of CuCl proved detrimental, confirming its essential role in the transformation.

One year later, the same group described a regioselective γ-C—C bond-forming strategy between diversely substituted cyclohexanone-derived silyl dienol-ethers **34** or isophorone-derived congeners **35** and α-halo carbonyl compounds **36**, furnishing the corresponding 1,6-dicarbonyl motifs **37** and **38** in good yields (54%–97% for **37** and 57%–85% for **38**, Scheme 8a) [33]. The researchers evaluated the ability of Cu(II) catalysts to activate α-halo carbonyls and generate the corresponding carbon-centered radicals, whose electron-poor philicity matches that of the π-system of the dienes [34]. This protocol proved to be applicable to a range of enone-derived silyl dienol ethers **34** featuring a distal, endocyclic γ-reactive site (e.g., compounds

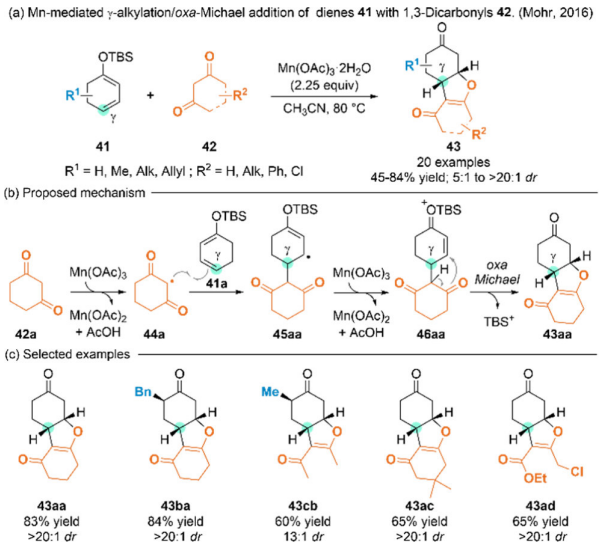


SCHEME 8 | Copper-catalyzed γ-alkylation of dienes **34** and **35** with α-ketoradical precursors **36**. PMDTA = pentamethyldiethylenetriamine; DBU = 1,8-diazabicyclo [5.4.0]undec-7-ene.

10990690, 0, Downloaded from https://chemistry-europe.onlinelibrary.wiley.com/doi/10.1002/ejoc.70753 by Claudio Curti - University Degli Studi Di Parma Stampa Universitaria Parmense , Wiley Online Library on [31/08/2026]. See the Terms and Conditions (https://onlinelibrary.wiley.com/terms-and-conditions) on Wiley Online Library for rules of use; OA articles are governed by the applicable Creative Commons License

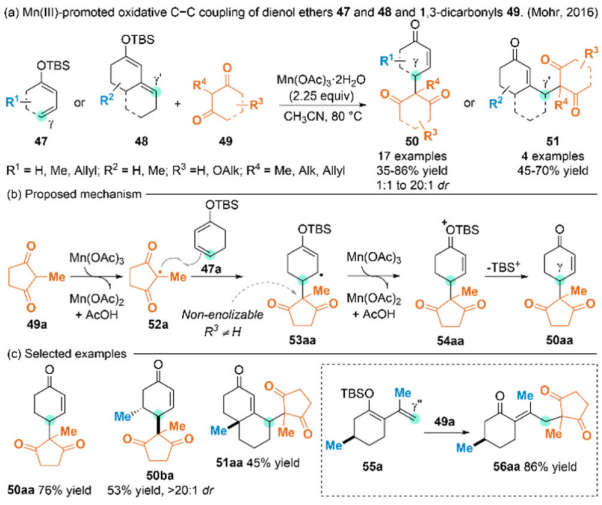
37aa–37ca, Scheme 8b); as well as to γ′-exocyclic congeners **35** (e.g., compounds **38aa–38ad**). Interestingly, the reaction proved viable also on a linear diene derivative incorporating a cyclopropyl group which reacted with ester **36a** to generate the corresponding γ-adduct **37da** in good yield (64%). The presence of alkyl or vinyl substituents within the six-membered ring of **34** and **35** did not hinder the reaction, resulting also in one highly diastereoselective entry, namely the predominantly *trans*-adduct **37ba** (Scheme 8b). The reaction tolerated several functional groups on the α-halo carbonyl partners **36**, including allylic motifs, amides, thioesters, and aldehydes. Finally, the authors demonstrated that the protocol could also be applied to a complex substrate such as the unprotected broad-spectrum antibiotic chloramphenicol (**39**), which served as radical precursor in the reaction with **35a** under the optimized reaction conditions, to furnish complex acrylamide **40** after workup with DBU (Scheme 8c).

In the same year, Mohr and coworkers developed a cascade γ-alkylation/*oxa*-Michael addition of preformed silyl dienol ethers **41**, exploiting the ability of $Mn(OAc)_3$ to oxidize 1,3-dicarbonyl compounds **42** and generate open-shell intermediates (Scheme 9a) [35]. This strategy enabled access to bicyclic or tricyclic products **43**, incorporating a dihydrofuran core, in moderate-to-good yields (45%–84%) and with complete regio- and diastereoselectivity, as only *cis* adducts were observed. The authors proposed that Mn(III) salt oxidized the 1,3-dicarbonyl **42a**, generating the electrophilic *C*-centered alkyl radical **44a**, which could react at the remote position of the electron-rich diene **41a**, furnishing the allylic open-shell intermediate **45aa** (Scheme 9b). The latter underwent a further Mn-promoted oxidation to give carbocation **46aa**, which then engaged in an intramolecular *oxa*-Michael reaction to deliver the final tricyclic scaffold **43aa** with complete *cis* diastereoselectivity. This strategy proved to be applicable to diversely substituted silyl dienol ethers **41** (entries **43aa–43cb**, Scheme 9c). Bulkier α′-substituents, such as the benzyl group (e.g., **43ba**), exhibited superior stereoinduction compared to their less hindered counterparts (**43cb**). In addition, various cyclic and acyclic 1,3-dicarbonyl compounds were evaluated, as exemplified by products **43ac** and **43ad**.



SCHEME 9 | Radical-mediated, γ-alkylation/*oxa*-Michael addition cascade to access *cis*-fused polycycles of type **43**.

In a related contribution, Mohr and coworkers expanded the utility of their Mn(III)-mediated oxidative processes by developing a remote C—C bond-forming protocol between dienol silanes of types **47** and **48** and a slight excess of α-substituted 1,3-dicarbonyl compounds **49** (Scheme 10a) [36]. Under the action of $Mn(OAc)_3{\cdot}2H_2O$ in acetonitrile at 80 °C, this strategy enabled access to a series of γ- or γ′-functionalized α,β-unsaturated ketones **50** and **51**, bearing a quaternary carbon center, in moderate-to-good yields (35%–86% for γ-adducts **50** and 45%–70% for γ′-adducts **51**) and with complete regioselectivity. Concerning the mechanism, as shown in Scheme 10b, the authors proposed that $Mn(OAc)_3$ initially oxidized the α-substituted 1,3-dicarbonyl substrate (e.g., **49a**), generating the electrophilic tertiary radical (e.g., **52a**), which could engage in a regioselective addition to the electron-rich SOMOphile (**47a**), furnishing an open-shell intermediate (e.g., **53aa**). Subsequent Mn-promoted oxidation delivered cationic species (**54aa**), which, after desilylation, afforded the final remotely functionalized product (**50aa**). It is important to note that, unlike the previously discussed case, the intramolecular *oxa*-Michael reaction was prevented here because the radical precursor lacked any enolizable protons at the α-position between the two carbonyl groups. The generality of this synthetic strategy was proven using various substituted silyl dienol ethers **47** and **48** with 1,3-dicarbonyl radical precursors **49** (Scheme 10c). Where the SOMOphile species bore a preexisting stereocenter proximal to the reactive site (e.g., **50ba**), high diastereoselectivity was observed (>20:1 *dr*). Also, stereoselectivity was excellent in a decalin system, with a single diastereomer of triketone **51ca** accessed albeit in a low 45% yield. Dienol ethers derived from terpenes, such as carvone, verbenone, and pulegone, were also tested: As an example, pulegone-derived silyl dienol ether **55a** reacted well with **49a** to afford the corresponding adduct **56aa** in a good 86% isolated yield with complete γ″-regioselectivity. Interestingly, the authors found that by using an excess of the silyl dienol ether relative to an α-unsubstituted precursor like 1,3-cyclohexandione, Meldrum's acid, or 1,3-indandione, a sequential double oxidation pathway was operative, enabling the addition of two molecules of the electron-rich diene yielding the corresponding α,α-doubly alkylated products (not shown).

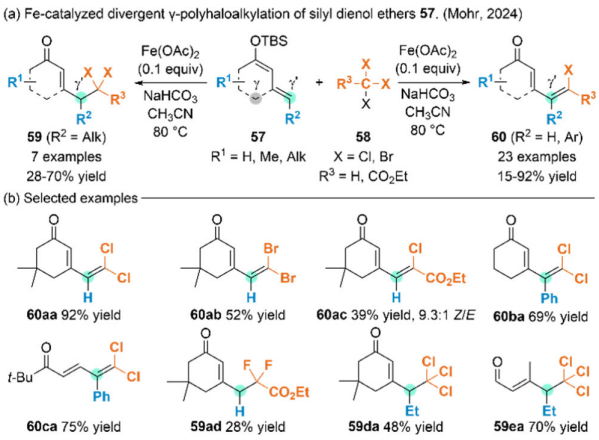


SCHEME 10 | Mn(III)-promoted remote C—C bond-forming protocol between dienol silanes **47** and **48** and α-substituted 1,3-dicarbonyl compounds **49**.

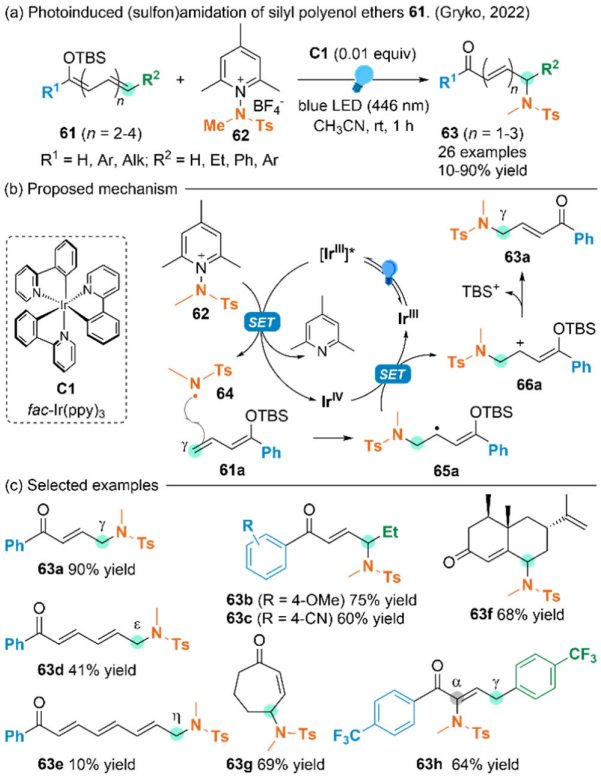
10990690, 0, Downloaded from https://chemistry-europe.onlinelibrary.wiley.com/doi/10.1002/ejoc.70753 by Claudio Curti - University Degli Studi Di Parma Stampa Universitaria Parmense , Wiley Online Library on [31/08/2026]. See the Terms and Conditions (https://onlinelibrary.wiley.com/terms-and-conditions) on Wiley Online Library for rules of use; OA articles are governed by the applicable Creative Commons License

More recently, in 2024, the same group reported a regioselective γ'-polyhaloalkylation of siloxydienes **57** in the presence of tetrahalomethanes or α,α,α-trihaloalkyl compounds **58** under Fe(II) catalysis (Scheme 11a) [37]. The reaction, carried out with a catalytic amount of $Fe(OAc)_2$ and $NaHCO_3$ in acetonitrile at 80 °C, afforded γ'-polyhaloalkyl or γ'-haloalkenyl α,β-unsaturated enones **59** and **60**, respectively, depending on the substitution pattern of the silyl dienol ether precursor **57**. The divergent reactivity observed suggested a two-step pathway involving a first γ-selective polyhaloalkylation of **57** to give adducts of type **59**, which in some cases could step forward to the corresponding halomethylene motifs **60**, via elimination of hydrogen halide. This behavior could be rationalized by assuming different acidities of either aliphatic or benzylic γ-proton after C—C bond formation. Substrates bearing an unsubstituted γ'-position ($R^2 = H$, e.g., **60aa**, **60ab**, **60ac**, Scheme 11b) or a γ'-aryl group (e.g., **60ba–60ca**) underwent rapid elimination, whereas γ'-alkyl counterparts showed slower elimination kinetics, likely due to the steric hindrance introduced by the substituent, which disfavored the optimal conformation required for β-elimination (e.g., **59da–59ea**). As an exception, the γ'-unsubstituted, difluoroalkylated product **59ad** did not undergo elimination, probably due to the scarce leaving group ability of the fluorine atom. Overall, this strategy enabled the preparation of seven enones of type **59** and 23 carbonyl compounds of type **60**, obtained in moderate-to-good yields (28%–70% and 15%–92%, respectively) and with complete regiocontrol at the exocyclic γ'-position.

In recent years, the growing interest in visible-light photoredox catalysis as an alternative platform for generating single-electron intermediates [38] has enabled the development of remote radical functionalization strategies for electron-rich π-extended silyl polyenol ethers and silyl ketene acetal congeners [7]. In 2022, Gryko and coworkers disclosed the regioselective (hyper)vinylogous, photocatalytic functionalization of both cyclic and linear silyl (poly)enol ethers of type **61** using *N*-aminopyridinium (Katritzky) salt **62** in the presence of the *fac*-Ir(ppy)$_3$ photocatalyst **C1** (Scheme 12a) [39]. The reaction, performed under blue-light irradiation (446 nm), enabled the remote (sulfon)amidation of a collection of 26 polyenol silanes, with production of the corresponding α,β-unsaturated carbonyl compounds **63** with low-to-good efficiency (10%–90% yield), yet with complete



SCHEME 11 | Divergent, γ'-polyhaloalkylation, or γ'-haloalkenylation strategy reported by the Mohr group.



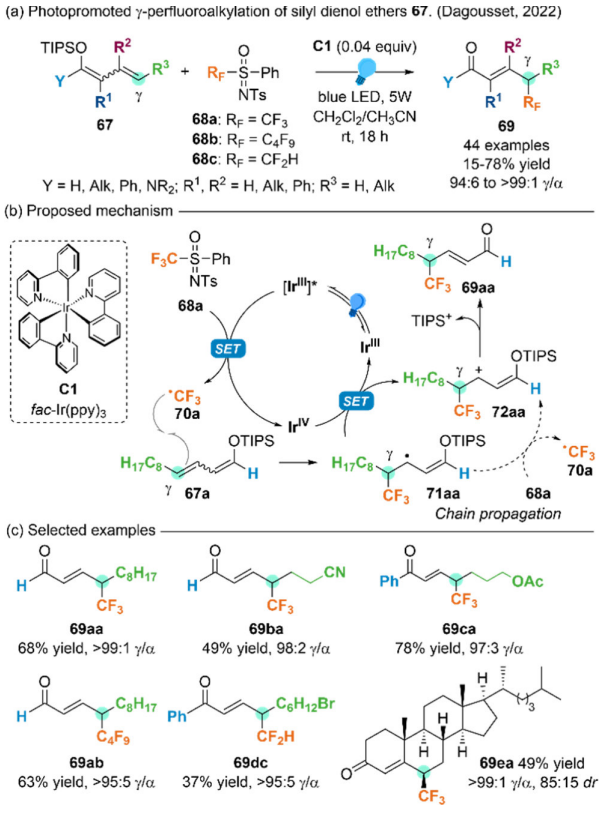
SCHEME 12 | Vinylogous and hypervinylogous photoinduced (sulfon)amidation of silyl (poly)enol ethers **61** developed by Gryko and coworkers. SET = single-electron transfer.

γ-regioselectivity. Concerning the proposed catalytic cycle (as exemplified by formation of **63a** in Scheme 12b), upon visible-light irradiation, the iridium(III)-based photocatalyst is promoted to its excited state $\mathbf{[Ir^{III}]^*}$, which is then able to reduce the N—N bond of aminopyridinium salt **62** through a SET process. This step generates the *N*-centered radical **64** (also backed up by control experiments) together with the oxidized $\mathbf{Ir^{IV}}$ species. This electrophilic open-shell intermediate subsequently engages with the electron-rich SOMOphile **61a** at the most distal position of the polyene chain, giving rise to the allyl radical **65a**. A second SET oxidation converts this radical into the corresponding carbocation **66a**, simultaneously regenerating the catalytically active $\mathbf{Ir^{III}}$ species. Finally, desilylation of **66a** furnishes the remotely functionalized product **63a**. The protocol proved broadly applicable to a variety of radical precursors and silyl dienol ethers, as illustrated by products **63a–c** (Scheme 12c). The methodology was further extended to hypervinylogous silyl tri- and tetraenol ethers, providing the polyunsaturated ε- and η-sulfonamido-derivatives **63d** and **63e**, albeit in lower yields. Furthermore, dienes derived from cyclic ketones also proved viable, as exemplified by the seven-membered enone **63g** which was secured in a good 69% isolated yield. The versatility of the developed reaction was also demonstrated in the late-stage functionalization of several biologically active compounds such as (+)-nootkatone which produced the γ-selective adduct **63f** in a moderate 68% yield. Interestingly, compounds bearing an electron-poor phenyl substituent (e.g., 4-CF_3Ph) undergo selective α-amidation using either silyl- or *O*-acetyl (not shown) dienol ether derivatives, giving the corresponding adducts (e.g., **63h**), as a single *Z*-diastereoisomer in moderate yields. Explanation of the exclusive remote functionalization was not provided at that time; however, these results fully

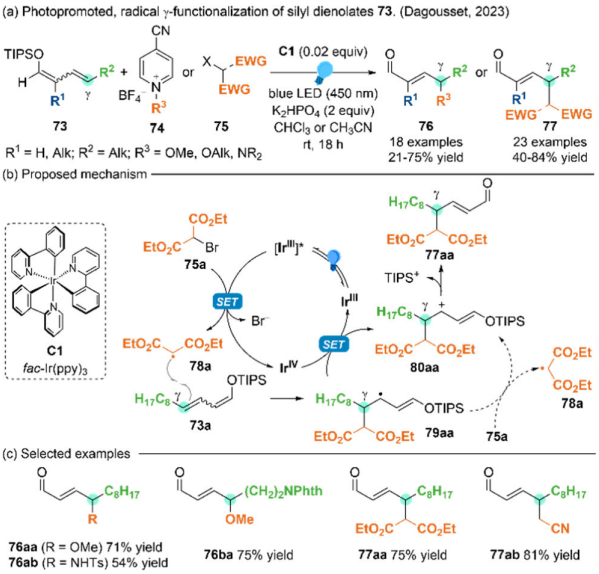
10990690, 0, Downloaded from https://chemistry-europe.onlinelibrary.wiley.com/doi/10.1002/ejoc.70753 by Claudio Curti - University Degli Studi Di Parma Stampa Universitaria Parmense , Wiley Online Library on [31/08/2026]. See the Terms and Conditions (https://onlinelibrary.wiley.com/terms-and-conditions) on Wiley Online Library for rules of use; OA articles are governed by the applicable Creative Commons License

match the rationalization recently given by Guo et al. (vide supra, Figure 2).

In the same year, Dagousset reported the remote perfluoroalkylation of aldehyde- and ketone-derived silyl dienol ethers **67** using perfluoroalkyl sulfoximines **68** as radical precursors and the iridium(III) photocatalyst **C1** (Scheme 13a) [40]. The reaction, performed in a 1:1 dichloromethane/acetonitrile mixture under blue-light irradiation (450 nm), afforded a quite large collection of γ-perfluoroalkylated α,β-unsaturated carbonyl compounds **69** in low-to-good yields (15%–78%) and with high remote regioselectivity (94:6 to > 99:1 γ/α). As shown in Scheme 13b for the preparation of **69aa** and based on the use of dienol silane **67a** and trifluoromethyl sulfoximine **68a**, the authors proposed a photocatalytic cycle where the excited photocatalyst **[Ir^{III}]*** reduces **68a** to generate the key, electrophilic trifluoromethyl radical **70a**. Thus, the addition of **70a** to the γ-position of diene **67a** delivers the open-shell, allyl radical **71aa**, which is first oxidized to carbocation **72aa** by **Ir^{IV}** (closing the cycle) and then readily desilylated to deliver product **69aa**. However, corroborated by a relatively high value of quantum yield ($\Phi = 0.25$), a radical chain mechanism was considered as a possible alternative: Indeed, oxidation of allyl radical intermediate **71aa** could arise at the expense of sulfoximine **68a**, whose reduction directly generates the required trifluoromethyl radical. As shown in Scheme 13c, this protocol enabled access to a variety of γ-trifluoromethyl α,β-unsaturated scaffolds, as well as remotely perfluoroalkylated derivatives bearing diverse substituents, including many complex biorelevant molecules.



SCHEME 13 | γ-Fluoroalkylation of vinylogous silyl dienol ethers **67** developed by Dagousset and coworkers. SET = single-electron transfer. Dashed arrows indicate a possible alternative/alongside mechanistic path.

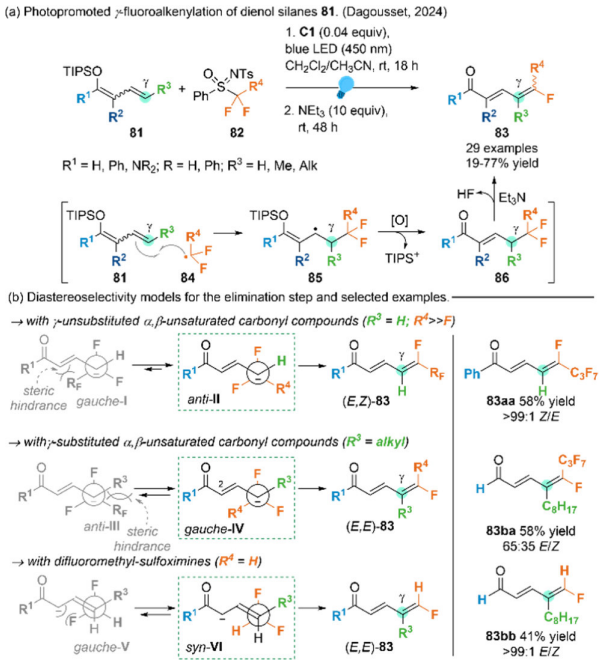


SCHEME 14 | Remote radical functionalization strategy of silyl dienol ethers **73** with several radical precursors **74** or **75** reported by Dagousset and coworkers. SET = single-electron transfer. Dashed arrows indicate a possible alternative/alongside mechanistic path.

Similarly, the same group introduced a photocatalytic strategy to selectively functionalize unbiased enals at their remote γ-position (Scheme 14a) [41]. To this end, they employed preformed silyl dienol ethers **73** together with diversely heteroatom-substituted *N*-aminopyridinium salts **74** or alkyl halides **75** as radical precursors, in the presence of catalytic amounts of *fac*-Ir(ppy)$_3$ **C1** (2 mol%) and K_2HPO_4. The reaction, carried out under blue-light irradiation (450 nm), furnished diverse γ-alkoxy or γ-amido α,β-unsaturated aldehydes **76** in 21%–75% isolated yield, along with diversely functionalized γ-alkylated enals **77** obtained in moderate-to-good yields (40%–84%) as racemates. In all cases, complete remote γ-regioselectivity was observed. The authors proposed a mechanistic pathway which is shown in Scheme 14b using the long-chain dienol ether **73a** and α-bromo diethylmalonate **75a**. As in the previously described photocatalytic transformations (Schemes 11 and 12), the excited photocatalyst **C1** undergoes an initial oxidative quenching by **75a**, generating the electrophilic carbon-centered radical **78a**. This open-shell species adds to the electron-rich SOMOphile **73a** to form allyl radical intermediate **79aa**, which is then oxidized to the corresponding carbocation **80aa** via regeneration of the photocatalyst. Desilylation of **80aa** finally delivers product **77aa**. Again, quantum yield measurements ($\Phi = 0.45$) indicated the presence of a short-chain radical pathway operating alongside the catalytic cycle, likely due to the ability of intermediate **79aa** to reduce diethyl bromomalonate **75a**, furnishing radical **78a**. As previously mentioned, the use of Katritzky salts **74** as radical precursors provided remotely alkoxylated or aminated enals (e.g., **76aa**, **76ab**, **76ba**, Scheme 14c), whereas alkyl halides **75** afforded the corresponding γ-alkylated products of type **77aa** and **77ab**.

Recently, Dagousset and coworkers reported a radical-mediated, vinylogous, one-pot two-step perfluoroalkylation/dehydrohalogenation protocol to access a series of differently substituted dienones and dienals of type **83** (Scheme 15a) [42]. Initially, perfluoroalkyl sulfoximines **82** were used as suitable radical

10990690, 0, Downloaded from https://chemistry-europe.onlinelibrary.wiley.com/doi/10.1002/ejoc.70753 by Claudio Curti - University Degli Studi Di Parma Stampa Universitaria Parmense , Wiley Online Library on [31/08/2026]. See the Terms and Conditions (https://onlinelibrary.wiley.com/terms-and-conditions) on Wiley Online Library for rules of use; OA articles are governed by the applicable Creative Commons License



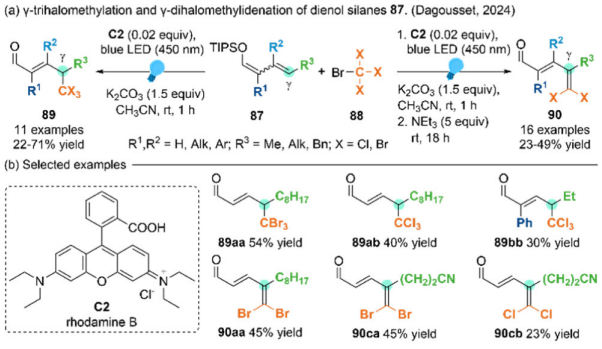
SCHEME 15 | One-pot, γ-perfluoroalkenylation/dehydroalogenation protocol to access fluorinated dienones and dienals of type **83**, developed by Dagousset et al.

precursors, which reacted with preformed silyl dienol ethers **81**, under blue-light irradiation (450 nm) in the presence of $Ir(ppy)_3$ (**C1**) to afford the corresponding γ-perfluoroalkylated adducts (vide infra). The subsequent addition of triethylamine enables the second elimination event which furnished the final products. A collection of 29 γ-perfluoroalkenylated α,β-unsaturated enals, enones, or amides **83** were thus obtained in low-to-good yields (19%–77%) with complete γ-regioselectivity. From a mechanistic point of view, in line with similar photocatalytic cycles, an electrophilic perfluoroalkyl radical **84**, generated from **82** by oxidative quenching of the excited photocatalyst **C1**, adds to the electron-rich silyl dienol ether **81** to generate the corresponding γ-functionalized α,β-unsaturated carbonyl compound **86** via the formation of the allyl radical intermediate **85** (Scheme 15a). Then, treatment of **86** with NEt_3 enables the dehydrohalogenation step affording the final diene **83**.

Interestingly, the diastereoselectivity of this second step heavily depended on the substitution pattern of both the diene **81** and the fluorinated reagent **82**, considering the process an $E1_{CB}$-type pathway involving formation of a transient dienolate intermediate, which undergoes fluoride elimination. To rationalize the observed diastereoselectivity and capitalizing on previous mechanistic studies for α-fluoroalkenylation of carbonyls [43], the authors proposed a series of open-chain models, as shown in Scheme 15b. For γ-unsubstituted diene **81** (R^3 = H) coupled with radical precursors **82** bearing a R^4 substituent bulkier than fluorine, the preferred conformation of the dienolate intermediate was the *anti*-conformer **II**, which resulted strongly favored over the *gauche* conformation **I**, and ultimately leading to the *Z* isomer (e.g., **83aa**). For substrates bearing an alkyl substituent at the γ-position of **81** (R^3 = alkyl), the diastereoselectivity decreased; in this instance, steric repulsion between R^3 and R_F in the conformer *anti*-**III** was slightly greater than that between R^3 and the $C(sp^2)$–2 of the α,β-unsaturated carbonyl fragment of the *gauche*-**IV** conformation, resulting in a modest preference for the latter, which confirmed the observed *E*-selectivity (e.g., **83ba**). Conversely, when unsubstituted radical precursors **81** (R^4 = H) were used, the similar size of hydrogen and fluorine atoms provided no steric discrimination. On the other hand, electronic factors, namely electrostatic repulsion between the F atom and the negatively charged dienolate destabilized conformer *gauche*-**V**, render conformer *syn*-**VI** more favorable, thus leading to the sole *E*-isomer (**83bb**).

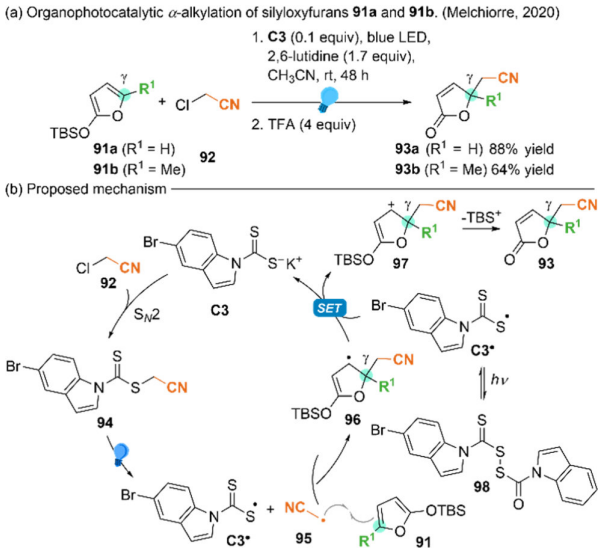
Building on their earlier contribution, the Dagousset group subsequently expanded this radical-based strategy to the trihalomethylation of enal-derived silyl dienol ethers **87** (Scheme 16a) [44]. In this study, the authors employed various tetrahalomethanes **88** as electrophilic radical precursors, in combination with rhodamine B (**C2**) as an organic dye photocatalyst and K_2CO_3 as the base. As shown in Scheme 16b, the reaction, carried out in acetonitrile under blue-light irradiation (450 nm), delivered a series of γ-trihalomethyl α,β-unsaturated enals **89** in poor-to-good yields (22%–71%) and with complete γ-regioselectivity (>20:1 in all entries). The process relied on the photoinduced generation of trihalomethyl radicals (not shown), which selectively engage the γ-position of electron-rich SOMOphiles **87**. Furthermore, a subsequent one-pot treatment with NEt_3 enabled access to 16 γ-dihalomethylidene α,β-unsaturated aldehydes **90** in moderate isolated yields (23%–49%).

In the context of a broad investigation on the photopromoted and organocatalyzed radical α-functionalization of diversely substituted silyl enol ethers, Melchiorre and coworkers reported, in a couple of entries, the regioselective γ-alkylation of silyloxyfurans **91a** and **91b** using chloroacetonitrile **92** as the radical precursor, 2,6-lutidine and the nucleophilic dithiocarbonyl anion organocatalyst **C3** (Scheme 17a) [45]. The reaction, performed in acetonitrile under blue-light irradiation, followed by acidic workup with trifluoroacetic acid, afforded the γ-functionalized α,β-unsaturated lactones **93a** and **93b** in 88% and 64% yields, respectively. The proposed mechanism is shown in Scheme 17b: First, the dithiocarbonyl anion **C3** performs a nucleophilic substitution (S_N2) on chloroacetonitrile **92**, generating the photon-absorbing intermediate **94**. Upon blue-light irradiation, photolytic cleavage of the C—S bond takes place, producing the open-shell species **C3**$^{\bullet}$ together with the electrophilic α-cyanoalkyl radical **95**. The latter selectively adds to the γ-position of the electron-rich silyloxyfuran **91**, forming the corresponding allyl radical intermediate **96**.



SCHEME 16 | Dagousset's organophotoredox approach to γ-trihalomethyl and γ-dihalomethylidene α,β-unsaturated enals **89** and **90**.

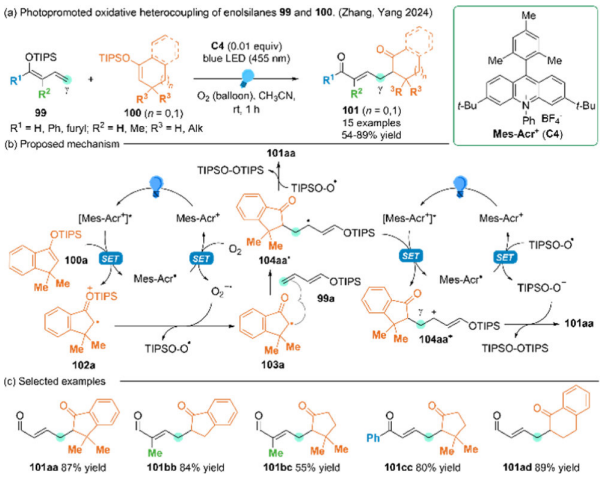
10990690, 0, Downloaded from https://chemistry-europe.onlinelibrary.wiley.com/doi/10.1002/ejoc.70753 by Claudio Curti - University Degli Studi Di Parma Stampa Universitaria Parmense , Wiley Online Library on [31/08/2026]. See the Terms and Conditions (https://onlinelibrary.wiley.com/terms-and-conditions) on Wiley Online Library for rules of use; OA articles are governed by the applicable Creative Commons License



SCHEME 17 | Radical, remote functionalization strategy of silyl ketene acetals **91a** and **91b** with chloroacetonitrile **92** promoted by nucleophilic, dithiocarbonyl anion organocatalyst **C3**. TFA = trifluoroacetic acid. SET = single-electron transfer.

A subsequent SET between **96** and the sulfur-centered radical **C3**$^{\bullet}$ regenerates the dithiocarbonyl anion **C3** furnishing the oxocarbenium ion **97**, which delivers the final products **93** upon desilylation. Quantum yield measurements ($\Phi = 0.05$) indicated that a radical chain pathway was highly unlikely, corroborating the closed catalytic cycle proposed by the authors. Interestingly, they suggested that the radical **C3**$^{\bullet}$ may also exist in equilibrium with its dimeric form **98**, a feature that could prolong catalyst lifetime, hence improving its turnover.

Shifting to a conceptually different study, in 2024, Zhang, Yang, and coworkers reported a metal-free, organophotoredox oxidative heterocoupling between π-extended silyl dienol ethers **99** and enol silanes **100** using Mes-Acr^{+}BF$_4^{-}$ (**C4**) as photocatalyst and molecular oxygen as the terminal oxidant (Scheme 18a) [46]. The reaction, performed in acetonitrile under blue-light irradiation (455 nm), furnished various γ-functionalized α,β-unsaturated carbonyl compounds **101** in moderate-to-high isolated yields (54%–89%) and with complete γ-regioselectivity. Supported by Stern–Volmer quenching experiments, the reaction relies on the observation that cyclic silyl enol ethers **100** are more readily oxidized by the excited photocatalyst than the corresponding linear vinylogous dienol silanes **99**. Together with electron paramagnetic resonance studies, indicating the formation of a superoxide radical intermediate, these findings informed the mechanistic proposal shown in Scheme 18b (as exemplified for the formation of **101aa**). Thus, upon blue-light excitation, the organic photocatalyst is promoted to its excited state [Mes-Acr^{+}]* which oxidizes silyl enol ether **100a** via SET, generating the radical cation **102a** and the corresponding acridine radical Mes-Acr$^{\bullet}$. The latter is then reoxidized by O_2, regenerating the photocatalyst and producing the superoxide anion $O_2^{\bullet-}$. Subsequently, desilylation of **101a** by $O_2^{\bullet-}$ affords the electrophilic α-keto radical **103a**, which is intercepted by the electron-rich SOMOphile **99a**. The observed γ-regioselectivity was rationalized by calculating the Gibbs free-energy difference between the transition states for radical addition at the γ-position ($\Delta\Delta G^{\ddagger} = 0$) of **99a** versus the α-position



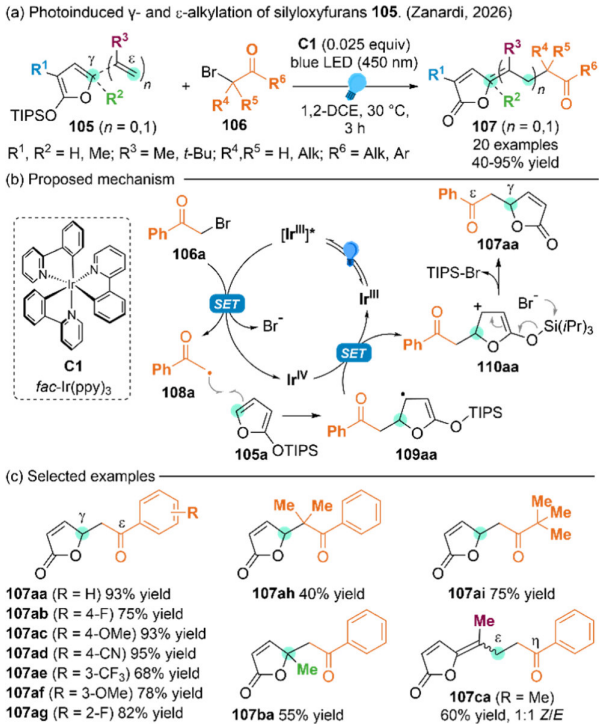
SCHEME 18 | Metal-free, organophotoredox oxidative heterocoupling between π-extended silyl dienol ethers **99** and enol silanes **100** to access 1,6-dicarbonyl compounds **101**. SET = single-electron transfer.

($\Delta\Delta G^{\ddagger} = 5.3$ kcal/mol), indicating a preference for γ-attack. The resulting radical intermediate **104aa**$^{\bullet}$ can then be oxidized by [Mes-Acr^{+}]* to form carbocation **104aa**$^{+}$, which undergoes desilylation to deliver the 1,6-dicarbonyl product **101aa**. An alternative pathway involving homolytic cleavage of the O—Si bond of **104aa**$^{\bullet}$ could not be ruled out by the authors. Overall, the protocol proved robust across a range of functionalized dienol silanes **99** and silyl enol ethers **100**, providing a diverse set of γ-functionalized α,β-unsaturated carbonyl compounds (e.g., **101aa**–**101ad**, Scheme 18c) with excellent remote regioselectivity.

Recently, our research group disclosed a photocatalytic and regioselective functionalization of silyloxyfurans **105** using α-bromo ketones **106** in the presence of *fac*-Ir(ppy)$_3$ (**C1**, Scheme 19a) [47]. The reaction, performed in 1,2-dichloroethane at 30 °C under blue-light irradiation (450 nm), delivered a collection of ε-keto-γ-butenolides **107** in moderate-to-good yields (40%–95%) and with complete remote regioselectivity. From a mechanistic standpoint, the excited photocatalyst **[Ir^{III}]*** undergoes a first, oxidative quenching with the α-bromo ketone **106a**, generating the electrophilic α-keto radical **108a** (Scheme 19b). This species then couples with the electron-rich SOMOphile **105a**, affording the open shell intermediate **109aa**. Further oxidation of this intermediate to the corresponding carbocation **110aa** regenerates the photocatalyst. Finally, the desired product **107aa** is secured by the prompt desilylation of **110aa**. As shown in Scheme 19c, this protocol proved effective across a range of substituted phenacyl bromides (products **107aa–107ag**), and aliphatic counterparts also performed well (**107ah–107ai**). Notably, the method enabled access to butenolide **107ba**, featuring a quaternary carbon atom in its γ-position. Extension of the strategy to hypervinylogous scaffolds further allowed selective ε-functionalization, as exemplified by molecule **107ca**.

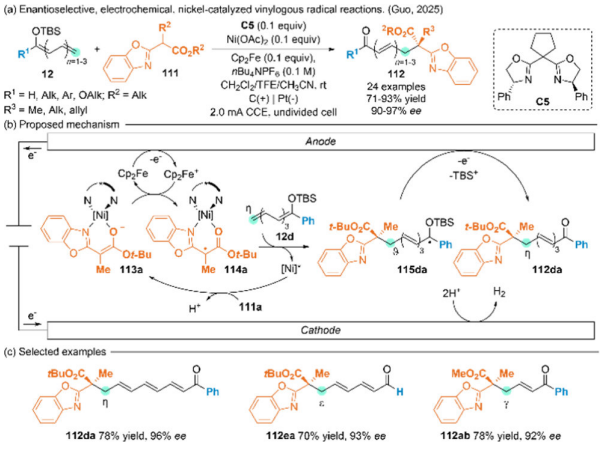
The renewed recent interest in synthetic electrochemistry as a direct means to generate single-electron intermediates [10] has opened additional and complementary avenues for remote radical functionalization of π-extended silyl polyenol ethers. In 2025, Guo and coworkers reported the first, enantioselective, electrochemical radical functionalization of vinylogous and hypervinylogous silyl polyenol ethers **12**, through their coupling with racemic

10990690, 0, Downloaded from https://chemistry-europe.onlinelibrary.wiley.com/doi/10.1002/ejoc.70753 by Claudio Curti - University Degli Studi Di Parma Stampa Universitaria Parmense , Wiley Online Library on [31/08/2026]. See the Terms and Conditions (https://onlinelibrary.wiley.com/terms-and-conditions) on Wiley Online Library for rules of use; OA articles are governed by the applicable Creative Commons License



SCHEME 19 | Photocatalytic, radical-mediated strategy to access ε- and η-keto-γ-butenolides **107** via remote alkylation of silyloxyfurans **105**. SET = single-electron transfer. DCE = 1,2-dichloroethane.

benzoxazolyl acetates **111** under nickel catalysis (Scheme 20a) [24]. The reaction, carried out in an undivided cell under constant current (2.0 mA, rt) in a CH_2Cl_2/2,2,2-trifluoroethanol/acetonitrile mixture, relied on the use of catalytic $Ni(OAc)_2$ and the chiral bis-oxazoline ligand **C5**, together with ferrocene (Cp_2Fe) as a redox mediator. Under these conditions, 24 remotely functionalized (poly)unsaturated carbonyl derivatives **112** were obtained in high yields (71%–93%) and high enantioselectivities (90%–97% ee), with a complete remote regiocontrol of the process. As shown in Scheme 20b for the preparation of **112da**, the authors proposed a catalytic cycle beginning with the condensation of benzoxazolyl acetate **111a** with the in situ generated chiral nickel complex from $Ni(OAc)_2$ and the enantiopure ligand



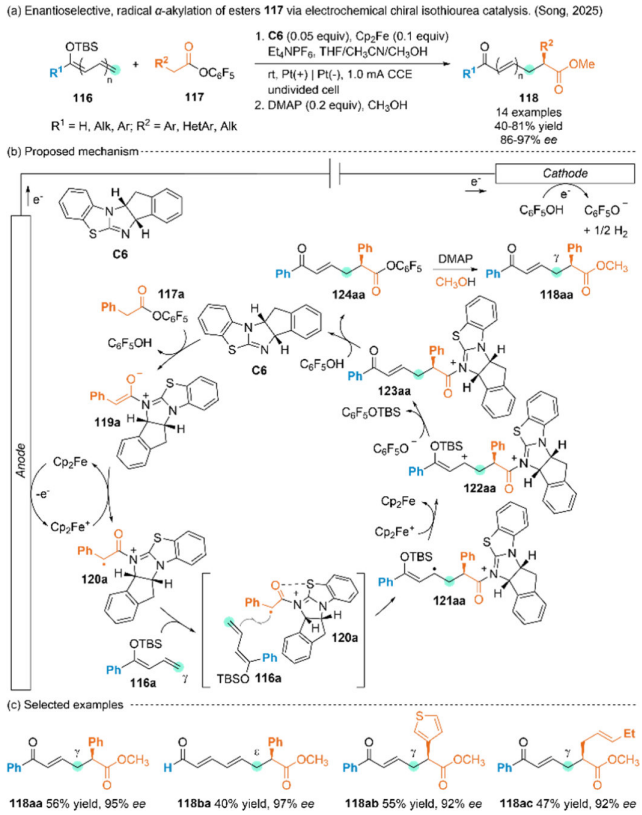
SCHEME 20 | Electrochemical enantioselective remote functionalization of silyl polyenol ethers **12** developed by Guo et al. Cp_2Fe = ferrocene. TFE = 2,2,2-trifluoroethanol.

C5, affording the chiral nickel-bound enolate **113a**. Meanwhile, Cp_2Fe (E_{onset} = +0.30 V) is oxidized to ferrocenium ion (Cp_2Fe^+) at the anode: Indeed, its small dimensions and high diffusiveness let it reach the electrode far more efficiently and in higher effective concentration than **113a** (E_{onset} = +0.21 V). The resulting Cp_2Fe^+ then selectively oxidizes the nickel-bound enolate **113a** to generate the α-alkoxycarbonyl radical **114a**, while simultaneously preventing the undesired direct oxidation of the electron-rich silyl tetraenol ether **12d** (E_{onset} = +0.63 V). The electrophilic radical **114a** then couples with electron-rich **12d** at the most remote site, forming the conjugated, ketyl-type intermediate **115da** regenerating the nickel catalyst. Finally, a second anodic oxidation event completes the sequence, delivering the remotely functionalized product **112da**. Representative examples, such as **112da**, **112ea**, and **112ab**, illustrate the efficiency and stereocontrol of this electrochemical manifold, consistently providing high yields and enantioselectivities across diverse substitution patterns (Scheme 20c). A thorough DFT-based investigation was performed, which provided a convincing and rare contribution to the rationalization of the remote regioselectivity invariably observed for these silyl polyenolates (see Figure 2 in this section).

In the same year, as part of a broader investigation into the enantioselective α-functionalization of silyl enol ethers, the Song group reported an electrochemical, asymmetric Lewis base-catalyzed strategy for the oxidative coupling of pentafluorophenyl esters **117** with silyl polyenolates **116** (Scheme 21a) [48].

The transformation was performed in an undivided cell under constant current (2.0 mA, rt) in a tetrahydrofuran/acetonitrile/methanol mixture, in the presence of ferrocene (Cp_2Fe) and a catalytic amount of the chiral isothiourea catalyst **C6**. Quenching the reaction with 4-dimethylaminopyridine (DMAP) in methanol gave access to a collection of diverse chiral and enantioenriched, remotely functionalized (poly)unsaturated carbonyl compounds **118** in moderate-to-high yields (40-81%), with good enantiocontrol (86%–97% ee) and complete remote regioselectivity. Here, the proposed mechanism includes a first nucleophilic acyl substitution of the chiral isothiourea catalyst **C6** to phenylacetic acid pentafluorophenyl ester **117a** generating the corresponding ammonium enolate **119a** (Scheme 21b, as exemplified for the synthesis of **118aa**). Anodic oxidation of **119a** mediated by Cp_2Fe^+ provides the electrophilic α-carbonyl radical **120a**, which undergoes a stereoselective addition to the π-bond of the electron-rich dienol silane **116a**, affording the corresponding allyl radical intermediate **121aa**. According to the authors' proposal, a weak, intramolecular interaction between the carbonyl oxygen and the sulfur atom of the chiral auxiliary restricts the conformational freedom of the open-shell intermediate **120a** enhancing the enantio-discrimination within the transition state of the coupling with **116a**. Further oxidation of **121aa** by Cp_2Fe^+ generates cationic species **122aa**, which, after desilylation, delivers the α,β-unsaturated carbonyl compound **124aa**, thus regenerating the catalyst. Finally, DMAP-mediated workup afforded the desired chiral γ-functionalized product **118aa**. The robustness of the protocol was demonstrated across a range of substituted acetic ester derivatives (products **118ab**–**118ac**) as well as hypervinylogous silyl polyenol ethers (**118ba**), consistently providing the corresponding products in moderate yields, with good enantiocontrol and complete regioselectivity (Scheme 21c). Finally, the use of silyl dienol ethers as electron-rich

10990690, 0, Downloaded from https://chemistry-europe.onlinelibrary.wiley.com/doi/10.1002/ejoc.70753 by Claudio Curti - University Degli Studi Di Parma Stampa Universitaria Parmense , Wiley Online Library on [31/08/2026]. See the Terms and Conditions (https://onlinelibrary.wiley.com/terms-and-conditions) on Wiley Online Library for rules of use; OA articles are governed by the applicable Creative Commons License



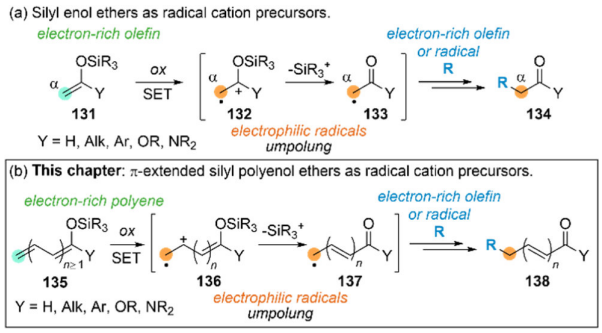
SCHEME 21 | Electrochemical, chiral isothiourea-catalyzed radical remote functionalization of π-extended silyl polyenol ethers **116** developed by Song and coworkers. Cp_2Fe = ferrocene. DMAP = 4-dimethylaminopyridine.

SOMOphile species in remote radical functionalization pathways has also been successfully exploited in the total synthesis of bioactive natural products, although only few examples have been documented so far (Scheme 22). In 2015, Yang and coworkers, in the context of their total synthesis of propindilactone G, reported an oxidative heterocoupling between cyclic enol silane **125** and acyclic silyl dienol ether **126** (Scheme 22a) [49]. The reaction was carried out in the presence of ceric(IV) ammonium nitrate and 2,6-di-*tert*-butylpyridine at low temperature in acetonitrile, delivering the desired intermediate **127** in an excellent 92% overall yield and complete remote regioselectivity as a mixture of diastereomers. More recently, in 2025, following their γ-polyhaloalkenylation strategy previously shown in Scheme 11, the Mohr group exploited the remote dibromoalkenylation of crotonaldehyde-derived silyl dienol ether **128** with tetrabromomethane **129** [50] in their efforts toward the total syntheses of panaxydiol and (–)-virol C; the transformation, catalyzed by $Fe(OAc)_2$, afforded the (*E*)−5,5-dibromopenta-2,4-dienal **130** in 69% isolated yield (Scheme 22b).

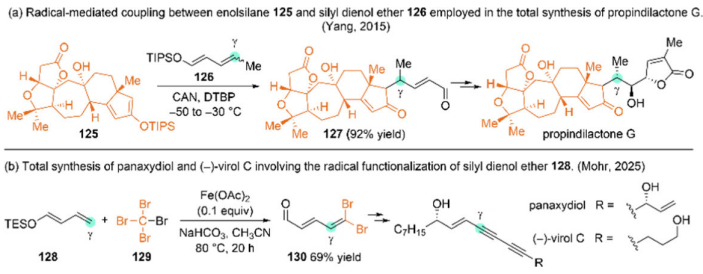
3 | Silyl Polyenol Ethers as Silyl Radical Cation Precursors

Within the radical chemistry domain, silyl enol ethers **131** (Scheme 23a) may be conveniently involved into a reactivity modality which is different, and often complementary, to that described in the previous section; indeed, these substrates can undergo facile single-electron oxidation to generate the corresponding radical cation species **132** [51]. This process constitutes an umpolung of their intrinsic polarity [52], as electron-rich enol silanes **131** are converted into electrophilic open-shell intermediates **132**. These species then may react either directly or, more commonly, undergo desilylation, to furnish the corresponding electrophilic α-keto radicals **133**. Once formed, intermediates **132** or **133** can engage in a variety of transformations, including quenching to regenerate the carbonyl precursor [53], intramolecular cyclization (For a seminal study on the intramolecular cyclization of silyl enol ethers promoted by a SET-oxidation, see: ref. [54]), coupling with suitable radical or olefin partners, ultimately delivering α-functionalized products **134**.

Although several transformations involving the single-electron oxidation of silyl enol ethers **131** have been disclosed, their vinylogous counterparts, namely the π-extended silyl polyenol



SCHEME 23 | Single-electron oxidation of enol silanes **131** and silyl polyenol ether congeners **135** providing access to the corresponding silyl radical cations. (a) Enol silanes **131** serving as electrophilic radical precursors. (b) Vinylogous silyl polyenol ethers **135** serving as electrophilic allyl radical precursors. SET = single-electron transfer.



SCHEME 22 | Application of remote radical functionalization strategies of vinylogous silyl polyenol ethers to the synthesis of natural products. (a) Total synthesis of propindilactone G developed by Yang and coworkers. (b) Total synthesis of panaxydiol and (–)-virol C reported by the Mohr group. CAN = ceric(IV) ammonium nitrate. DTBP = 2,6-di-*tert*-butylpyridine.

10990690, 0, Downloaded from https://chemistry-europe.onlinelibrary.wiley.com/doi/10.1002/ejoc.70753 by Claudio Curti - University Degli Studi Di Parma Stampa Universitaria Parmense , Wiley Online Library on [31/08/2026]. See the Terms and Conditions (https://onlinelibrary.wiley.com/terms-and-conditions) on Wiley Online Library for rules of use; OA articles are governed by the applicable Creative Commons License

ethers and silyl ketene acetals **135** (Scheme 23b), remain scarcely explored, despite their lower oxidation potentials (vide infra), and the increased molecular complexity readily accessible from such vinylogous substrates. Paralleling the above-mentioned pathway, single-electron oxidation of polyenes **135** generates the corresponding silyl radical cations **136**, here deployed as the conjugated counterparts of **132**. Radicals **136** might then react as such or lose the silyl group to afford the corresponding allyl keto radical intermediate **137**. Either electrophilic radicals **136** and **137** might then be coupled with an electron-rich olefin or another radical species to forge remotely functionalized adducts **138**. As often occurring in processes involving π-extended systems, several issues related to the regio- and stereocontrol of the reactions arise, making the development of these processes more challenging. Herein, we are going to discuss the few reports published on this matter so far, not before providing some background on the oxidation potentials of these electron-rich polyenes, their umpolung reactivity, and the regioselectivity issues arisen with their use. Systematic studies examining how the redox properties of enol silanes correlate with their structural features are still rare; however, an important early contribution came from Fujita and coworkers, who in 1992 calculated the oxidation potentials (E^0_{ox}) of a series of diversely substituted silyl enol ethers and silyl ketene acetals using the Rehm–Weller Gibbs energy relationship (Figure 3a–c, compounds **131a–f**) [55, 56]. Close analysis of these data, which confirm the intrinsic susceptibility of silyl enol ethers toward oxidation ($E_{ox} < 1.35$ V), also reveals that the oxidation potential is significantly influenced by the substitution pattern of the enolate. For instance, the dimethyl-substituted silyl ketene acetal **131a** displayed an E^0_{ox} value of +0.83 V (vs. SCE), its monomethyl analogue **131c** + 1.05 V (vs. SCE), and the unsubstituted trimethylsilane **131e** a value of +1.28 V (vs. SCE). A similar trend was observed when comparing the disubstituted silane **131b** (E^0_{ox} vs. SCE) with the monosubstituted counterpart **131d** (E^0_{ox} = +1.30 V vs. SCE). The unsubstituted trimethyl [(1-phenylvinyl)oxy]silane **131f** exhibited an oxidation potential of +1.32 V (vs. SCE). Authors attributed this trend to the electron-donating effect of alkyl substituents through hyperconjugation

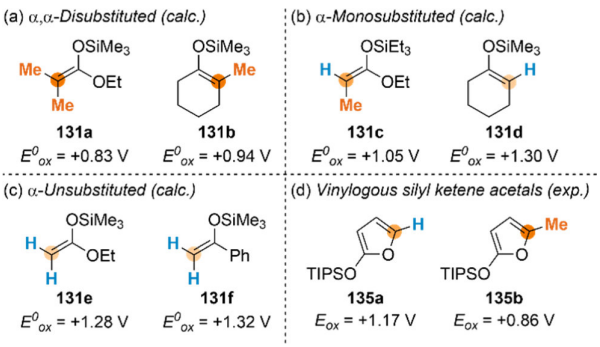


FIGURE 3 | Oxidation potentials (E_{ox}) of a selection of diversely substituted silyl enol ethers and silyl ketene acetals. (a) Fujita's calculated potentials of α,α-disubstituted silyl ketene acetal **131a** and cyclic silyl enol ether **131b**. (b) Fujita's calculated potentials of α-monosubstituted silyl ketene acetal **131c** and cyclic silyl enol ether **131d**. (c) Fujita's calculated potentials of unsubstituted silyl ketene acetal **131e** and silyl enol ether **131f**. (d) Curti's experimental potentials of unsubstituted silyloxyfuran **135a** and γ-methyl silyloxyfuran **135b** (V vs. Ag pseudoreference). Calc. = calculated; Exp. = determined by cyclic voltammetry.

(A similar trend was experimentally confirmed also for several highly congested silyl enol ethers and a series of tetralone-derived congeners. See, for example: ref. [55, 57]).

Passing to π-extended silyl polyenol ethers, even less data are still available. Recently, in a work carried out by our research group (vide infra), the redox properties of vinylogous silyloxyfurans **135a** and **135b** were experimentally determined by cyclic voltammetry measurements (Figure 3d) [58]. Consistent with Fujita calculations, the γ-methyl-substituted triisopropyl((5-methylfuran-2-yl)oxy)silane **135b** showed an E_{ox} of +0.86 V (vs. Ag pseudoreference), whereas its γ-unsubstituted analogue **135a** displayed a higher oxidation potential of +1.17 V (vs. Ag pseudoreference) [58]. In the same study, DFT calculations were also carried out to investigate the electronic distribution of triisopropylsilyloxy furan **135a** and its corresponding radical cation **136a** (Figure 4) [58]. Global and local nucleophilicity (N) and electrophilicity (ω) indices were first evaluated to assess the intrinsic reactivity of the two species. The silyl radical cation **136a** emerged as an amphiphilic intermediate, with a more pronounced electrophilic character ($\omega_0 = 8.5$ vs. $N_0 = 7.1$). Conversely, the silyl ketene acetal precursor **135a** displayed a marked nucleophilic profile ($\omega_0 = 0.7$ vs. $N_0 = 3.3$), thus corroborating the umpolung reactivity upon switching from HOMO- to SOMO-controlled transformations.

Also, to rationalize the regioselectivity behavior of these silyloxy furans when engaged in single-electron oxidations (vide infra), the SOMO composition, spin-density distribution, and condensed Fukui indices (f_0) at the radical centers of triisopropylsilyloxy radical cation **136a** (Figure 4b) were examined. The analysis showed that the radical center is preferentially located at C5 (γ-position, spin density = 0.4351, $f_0 = 0.1898$), but C3 (α-position) can also accommodate the single-electron character (spin density = 0.2070, $f_0 = 0.1354$). This distribution accounted for the experimentally observed slight preference for γ-addition, while still allowing for competitive reactivity at the α-position (see Scheme 27).

To the best of our knowledge, the first contribution based on a SET oxidation of silyl dienol ethers to generate the corresponding radical cation species dates back to 1993, when Ruzziconi and coworkers reported a cerium(IV) ammonium nitrate

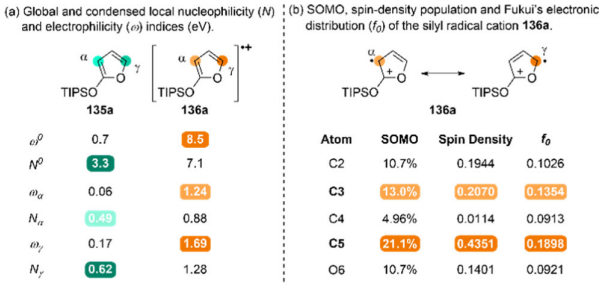
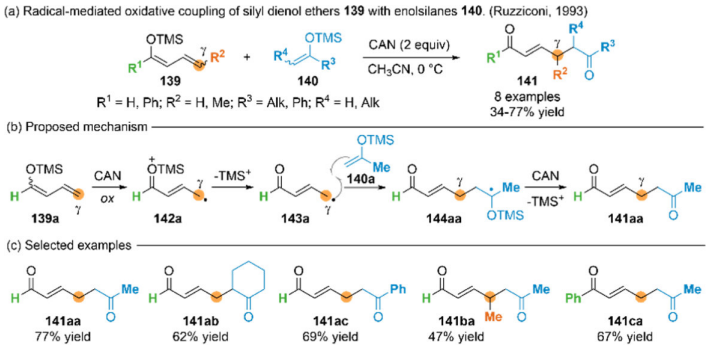


FIGURE 4 | DFT calculations of silyloxy furan **135a** and radical cation intermediate **136a**. (a) Calculated global and condensed local electrophilicity and nucleophilicity indices. N_0 = global nucleophilicity index (eV); ω_0 = global electrophilicity index (eV). N_α, N_γ = condensed nucleophilicity indices relative to C3 (α) and C5 (γ), respectively. (b) Analysis of SOMO, spin density, and Fukui's electronic distribution of radical cation **136a**.

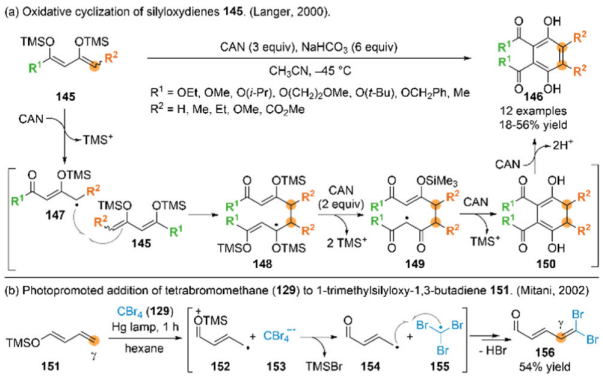
10990690, 0, Downloaded from https://chemistry-europe.onlinelibrary.wiley.com/doi/10.1002/ejoc.70753 by Claudio Curti - University Degli Studi Di Parma Stampa Universitaria Parmense , Wiley Online Library on [31/08/2026]. See the Terms and Conditions (https://onlinelibrary.wiley.com/terms-and-conditions) on Wiley Online Library for rules of use; OA articles are governed by the applicable Creative Commons License



SCHEME 24 | Radical-mediated oxidative coupling of silyl dienol ethers **139** with enol silanes **140** developed by Ruzziconi and coworkers. CAN = ceric (IV) ammonium nitrate.

(CAN)-mediated oxidative addition of linear silyloxy dienes **139** to ketone-derived silyl enol ethers **140** (Scheme 24a) [59].

The reaction, performed in acetonitrile at 0 °C, afforded a series of α,β-unsaturated 1,6-dicarbonyl compounds **141** in moderate-to-good yields (34%–77%) and with complete remote regioselectivity. The authors proposed a mechanism based on the higher tendency toward oxidation of π-extended silyl dienol ethers **139** compared to their nonvinylogous counterparts **140**. Accordingly, as shown in Scheme 24b for the formation of **141aa**, single-electron oxidation of dienol silane **139a** by CAN generates the corresponding silyl radical cation **142a** which, after desilylation, furnishes the conjugated γ-carbonyl radical **143a**. This electrophilic radical then attacks the electron-rich SOMOphile **140a**, generating the open-shell intermediate **144aa**. Finally, a second, CAN-promoted oxidation/desilylation sequence delivers the desired α,β-unsaturated 1,6-dicarbonyl product **141aa** with full remote regioselectivity. The mechanistic proposal was supported by the experimental observation that a significant excess (up to 10 equivalents) of silyl enol ethers **140** was required to suppress the formation of the undesired homocoupling by-product of silyloxy dienes **139**. Moreover, the authors attributed the observed regioselectivity to the greater stability of the conjugated γ-radical **143a** compared to its nonconjugated α-radical resonance form (not shown). This protocol proved applicable to a variety of substituted silyl dienol ethers and enol silanes (e.g., **141aa–141ca**, Scheme 24c). Notably, the remote regioselectivity was still observed even on γ-substituted silyl dienol ether (e.g., **141ba**). In 2000, Langer reported a regioselective entry to functionalized 1,4-dihydroquinones of type **146** via a CAN-mediated oxidative dimerization/cyclization of 1,3-bis(trimethylsilyloxy)buta-1,3-dienes **145** in the presence of $NaHCO_3$ (Scheme 25a) [60]. The reaction, performed in acetonitrile at –45 °C, afforded a series of differently substituted 1,4-hydroquinones **146** in low-to-moderate yields (18%–56%). According to the authors, the process is initiated by a CAN-mediated SET oxidation of the silyl dienol ethers **145**, generating the corresponding silyl radical cations (not shown). Subsequent monodesilylation furnishes radical intermediates **147**, which can add to another molecule of diene **145** at its remote γ-position. The resulting open-shell species **148** then undergo a double CAN-promoted oxidation/desilylation sequence, giving radicals **149**. These intermediates cyclize and, after an additional oxidation step, deliver scaffolds **150**, which are finally oxidized by CAN to the hydroquinone products **146**.



SCHEME 25 | Seminal examples of single-electron oxidation of silyl dienol ethers to their corresponding radical cations. (a) Oxidative cyclization of siloxydienes **145** to hydroquinone derivatives **146**. (b) Photopromoted, vinylogous dibromoalkenylation of diene **151** to reach brominated dienal **156**. CAN = cerium (IV) ammonium nitrate.

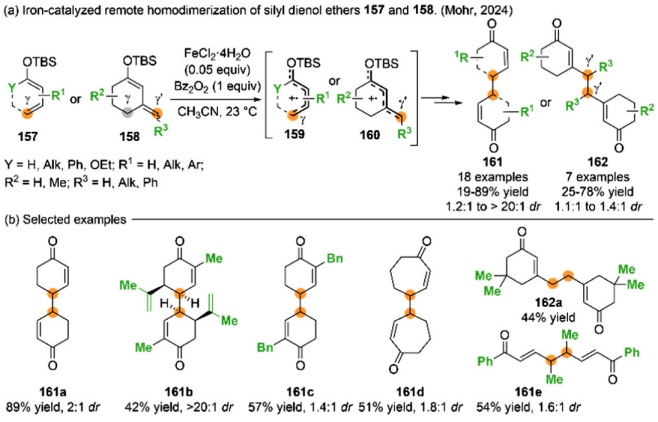
Within a broader investigation on a photopromoted radical addition of polyhalides to ketene silyl acetals and silyl enol ethers, the Mitani group reported a single example of a remote dibromomethylenation of enal-derived 1-trimethylsilyloxy-1,3-butadiene **151** with CBr_4 (Scheme 25b) [61]. The reaction, carried out in hexane in the presence of tetrabromomethane **129** and irradiated with a Hg lamp for 1 h, afforded the 5,5-dibromopenta-2,4-dienal **156** in 54% isolated yield as a single γ-regioisomer. From a mechanistic standpoint, the authors proposed that Hg-lamp irradiation triggers a photoinduced electron transfer between the silyl dienol ether **151** and tetrabromomethane **129**, generating the corresponding silyl radical cation **152** and brominated radical anion **153** species. Subsequent desilylation and debromination of **152** and **153**, respectively, furnish the allyl radical intermediate **154** and the tribromomethyl radical **155**, which couple together providing a α,β-unsaturated γ-tribromomethyl intermediate (not shown). A final dehydrobromination step delivers the desired 5,5-dibromopenta-2,4-dienal **156**. More recently, in 2024, Mohr and coworkers reported an Fe(II)-catalyzed oxidative homodimerization of silyl dienol ethers **157** and **158** (Scheme 26) [62], affording a collection of α,β-unsaturated enone dimers **161** and **162** in low-to-high yields (19%–89%), with complete remote regioselectivity and variable diastereocontrol (1.1:1 to > 20:1 *dr*).

The reaction, performed in acetonitrile at 23 °C using benzoyl peroxide and a catalytic amount of $FeCl_2{\cdot}4H_2O$ as the oxidant

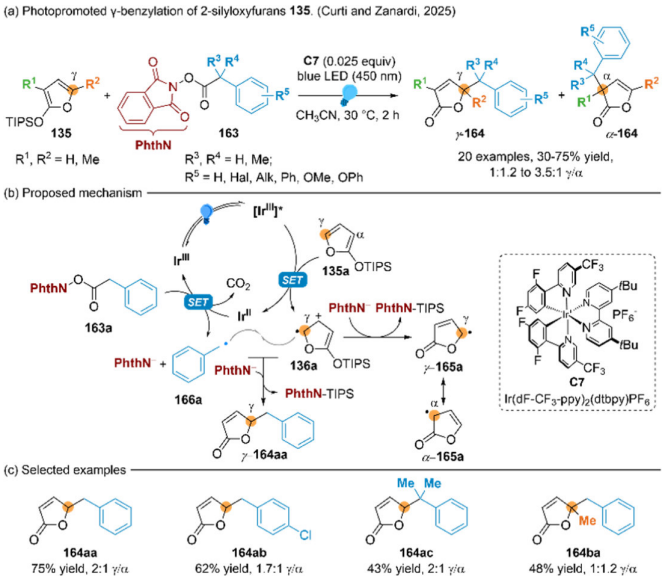
10990690, 0, Downloaded from https://chemistry-europe.onlinelibrary.wiley.com/doi/10.1002/ejoc.70753 by Claudio Curti - University Degli Studi Di Parma Stampa Universitaria Parmense , Wiley Online Library on [31/08/2026]. See the Terms and Conditions (https://onlinelibrary.wiley.com/terms-and-conditions) on Wiley Online Library for rules of use; OA articles are governed by the applicable Creative Commons License

couple, starts with the oxidation of silyl dienol ethers **157** or **158** to the corresponding radical cations **159** or **160** (Scheme 26a). These intermediates undergo γ,γ- or γ',γ'- radical–radical homocoupling to forge the new C—C bond, followed by desilylation to deliver the final products **161** or **162**, respectively. As shown in Scheme 26b, the protocol proved broadly applicable to endocyclic (e.g., **161a–161d**), exocyclic (e.g., **162a**), and linear (e.g., **161e**) silyl dienol ethers, consistently providing the corresponding α,β-unsaturated carbonyl dimers. Notably, the dienol silane derived from carvone furnished product **161b** as a single diastereomer. Recrystallization from hexanes afforded X-Ray quality crystals, enabling unambiguous assignment of the relative configuration at the ring junction of this endocyclic dimer. The formation of new carbon–carbon bonds through radical–radical coupling might also offer a valuable complementary strategy to the previously described approaches. This is because radical–radical couplings circumvent philicity mismatch issues, which typically hinder reactions between a radical and a neutral SOMOphile species that share the same electronic character, whether both are predominantly electrophilic or predominantly nucleophilic. By engaging two open-shell intermediates, this strategy enables efficient bond formation even in cases where traditional polarity-guided coupling fails. In this context, we have recently introduced the first, photopromoted γ-benzylation of silyloxyfurans **135** in the presence of *N*-(arylacetoxy)phthalimides **163** as benzyl radical precursors (Scheme 27a) [58]. Under irradiation with blue LEDs (450 nm) in acetonitrile and employing Ir(dF-CF_3-ppy)$_2$(dtbbpy)PF_6 (**C7**) as photocatalyst, the reaction proceeded smoothly at 30 °C for 2 h to afford a collection of γ-benzyl butenolides **164**, in overall moderate-to-good yields (30%–75%) and variable γ/α ratio. To rationalize the observed couplings, we proposed a photocatalytic cycle supported by Stern–Volmer measurements, on–off experiments, and quantum yield determination ($\Phi = 0.02$) as shown in Scheme 27b for the preparation of **164aa**.

Key to the maneuver is the single-electron oxidation of silyloxyfuran **135a** by the photoexcited $[Ir^{III}]^*$ species to provide the conjugated silyl radical cation **136a** whose electrophilic character (see Figure 4) determines an umpolung of the silyloxyfuran reactivity. Intermediate **136a** may either engage directly in subsequent steps or undergo rapid desilylation (facilitated by CH_3CN [53] or by the phthalimide anion $PhthN^-$), to afford the furanone radical



SCHEME 26 | Fe-Catalyzed oxidative γ,γ- or γ',γ'-dimerization of silyl dienol ethers **157** or **158** developed by Mohr and coworkers. Bz_2O_2 = benzoyl peroxide.



SCHEME 27 | Photopromoted γ-benzylation of 2-silyloxyfurans **135** with radical precursors **163** reported to afford γ-benzylbutenolides **164**. SET = single-electron transfer.

γ-**165a** or its mesomeric form α-**165a**. The allyl radical species **165a** or radical cation **136a** then couples with the nucleophilic benzyl radical **166a**, which is formed in situ via the Ir^{II} mediated single-electron reduction of the *N*-(phenylacetoxy)phthalimide **163a**, which completes the catalytic cycle, regenerating the photocatalyst. This protocol proved effective across a range of diversely substituted silyl ketene acetals **135** and *N*-(arylacetoxy)phthalimides **163**, delivering the desired γ-benzyl butenolides (e.g., **164aa–164ba**, Scheme 27c), together with minor amounts of the corresponding α-benzyl regioisomers. Interestingly, when γ-methyl silyloxyfuran **135b** was used in combination with benzyl radical precursor **163a** (not shown), the regioisomeric ratio of the corresponding adduct **164ba** was reversed in favor of the α-adduct (1:1.2 γ/α), indicating that steric and/or electronic effects at this site can redirect the benzyl radical attack. In this work, as already shown in Figure 4, thorough DFT calculations were carried out to investigate the electronic distribution of silyloxy furans of type **135** and their corresponding radical cation species. These studies corroborated the proposed umpolung reactivity upon switching from HOMO- to SOMO-controlled transformations of these silyloxyfurans and accounted for the observed γ- versus α- regioselectivity of the transformation. Finally, the reaction proved unsuited for electron-rich, 4-methoxy-, and 4-phenoxybenzyl radical precursors, which provided the corresponding adducts in meager 30%–35% combined yields in a 2.5:1 γ/α ratio (not shown). Being the hydroxybenzyl moiety a group embedded in many biorelevant phenyl γ-valerolactone metabolites [63], the inferior performance observed for these specific substrates led the author to seek different options to succeed (vide infra, Scheme 29).

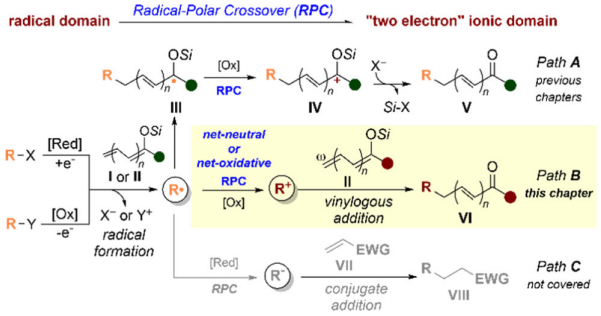
4 | Silyl Polyenol Ethers as Nucleophilic Partners in Radical–Polar Crossover Processes

As illustrated in the previous sections, radical chemistry merged with vinylogous nucleophilic systems has emerged as a highly

10990690, 0, Downloaded from https://chemistry-europe.onlinelibrary.wiley.com/doi/10.1002/ejoc.70753 by Claudio Curti - University Degli Studi Di Parma Stampa Universitaria Parmense , Wiley Online Library on [31/08/2026]. See the Terms and Conditions (https://onlinelibrary.wiley.com/terms-and-conditions) on Wiley Online Library for rules of use; OA articles are governed by the applicable Creative Commons License

versatile tool in contemporary organic synthesis. Indeed, the intrinsic reactivity of open-shell species, combined with the synthetic versatility of π-extended systems, enables the rapid assembly of complex architectures from simple starting materials. Notably, radical transformations often proved complementary to polar ones, further enriching the synthetic strategies at the chemist's disposal. The convergence of radical and polar processes within a single, conceptual framework is therefore particularly compelling, as it would unlock novel mechanistic opportunities to build connections between radical species and polar reaction partners. In this context, RPC refers to a class of reactions in which an open-shell radical intermediate R•, generated via either oxidation or reduction of suitable precursors (R-X or R-Y, Scheme 28) by way of chemical, photoredox, or electrochemical tools, is subsequently converted back into the two-electron ionic reaction manifold through single-electron oxidation or reduction (Scheme 28, Paths A-C) [64, 65]. In the second section of this review, we described a general mechanistic scenario in which electron-rich, vinylogous silyl polyenol ethers **I** or silyl ketene acetal congeners **II** intercepted an electrophilic radical at the most remote position, leading to the formation of an allyl radical intermediate **III** (Scheme 28, Path A). Subsequent oxidation of this intermediate to the corresponding carbocation **IV**, followed by desilylation, could furnish the final products **V**. The shift from the radical domain to the "two-electron" ionic domain exemplified by the latter oxidation step represents a RPC event.

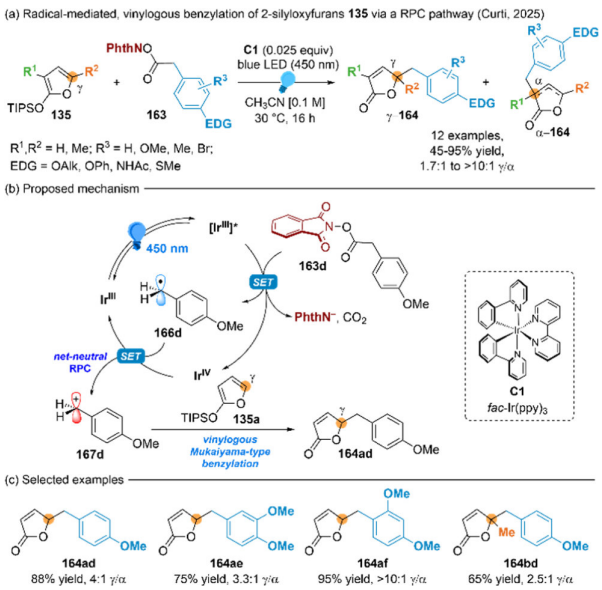
Regarding the radical-mediated vinylogous reactivity of silyl polyenolates, alternative RPC approaches have been developed that rely on generating electrophilic species—primarily carbocations R^+—through the single-electron oxidation of a parent radical R• (Scheme 28, Path B). This transformation is considered "*net-neutral*" when the oxidation is carried out by the same (photo)catalyst responsible for the initial reductive formation of R• [64]; conversely, it becomes a "*net-oxidative*" RPC when both the radical and the resulting carbocation arise from two separate oxidative events [66]. These complementary RPC pathways preserve the inherent polar behavior of vinylogous polyenol ethers, yet broaden the range of compatible reaction partners, including electrophiles that are difficult to access under purely polar conditions (e.g., imines and iminium ions, vide infra). A third RPC scenario—where the radical R• is instead reduced to the corresponding anion R^-, which then undergoes conjugate addition to suitable Michael acceptors **VII** to afford adducts **VIII** (Scheme 28, Path C)—lies beyond the scope of this review and will not be covered here [67]. A recent, net-neutral RPC-based strategy was assessed by Curti, Zanardi



SCHEME 28 | General overview of RPC pathways involved in radical-mediated, vinylogous transformations. *Si* = SiR_3.

and coworkers as a complementary option to the previously described photopromoted, vinylogous, Mukaiyama-type benzylation of silyloxyfurans **135** with radical precursors **163**, via a radical–radical coupling (Scheme 29) [58]. The aim of this study was to identify a second protocol capable of enabling the reaction between **135** and electron-rich *N*-(arylacetoxy)phthalimides **163**, bearing one or more electron-donating substituents at the aromatic ring, which had shown limited reactivity under the previous conditions. After a brief optimization, the authors found that irradiation with blue light (450 nm) under slightly modified reaction conditions (MeCN at 30 °C for 16 h), enabled *fac*-Ir(ppy)$_3$ (**C1**) to efficiently catalyze the reaction. A panel of twelve γ-benzylbutenolides **164** was accessed in moderate-to-high yields (45%–95%), with improved γ/α regioselectivity ratios (1.7:1 to > 10:1 γ/α, Scheme 29a).

The reaction was effective across a variety of electron-rich derivatives, including mono-, di-, and trisubstituted benzyl radical precursors of type **163**. Among them, phthalimide **163f**, featuring a 2,4-dimethoxyphenyl substituent, delivered the best outcome, affording the γ-adduct **164af** in 95% isolated yield as a single regioisomer (γ/α > 10:1, Scheme 29c). In contrast, the unsubstituted *N*-(phenylacetoxy)phthalimide and several electron-poor analogues—as the 4-bromophenyl derivative (not shown)—failed to react with **135**, prelude of a mechanistic pathway distinct from, yet complementary to the previously described radical–radical coupling process. Consistent with this proposal, Stern–Volmer analyses, on/off and appropriate control experiments—together with the low measured quantum yield (Φ = 0.05)—supported a new photocatalytic cycle incorporating a net-neutral RPC pathway. As shown in Scheme 29b for the preparation of the 4-methoxyphenyl derivative **164ad**, the catalytic sequence begins with the decarboxylative reduction of **163d** (E_{red} = −1.46 V vs. Ag pseudoreference) by the photoexcited complex **C1** (E^*_{red} = −1.73 V vs. SCE). This reduction furnishes the 4-methoxybenzyl radical **166d**, which is subsequently



SCHEME 29 | Radical-mediated, vinylogous Mukaiyama-type benzylation of silyloxyfurans **135** with electron-rich phthalimide esters **163** by way of a net-neutral RPC strategy. EDG = electron-donating group. SET = single-electron transfer.

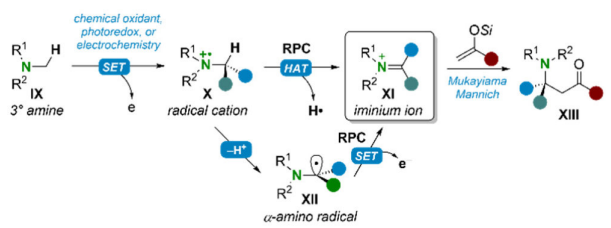
10990690, 0, Downloaded from https://chemistry-europe.onlinelibrary.wiley.com/doi/10.1002/ejoc.70753 by Claudio Curti - University Degli Studi Di Parma Stampa Universitaria Parmense , Wiley Online Library on [31/08/2026]. See the Terms and Conditions (https://onlinelibrary.wiley.com/terms-and-conditions) on Wiley Online Library for rules of use; OA articles are governed by the applicable Creative Commons License

oxidized to the corresponding benzyl carbocation **167d**, a RPC step facilitated by the electron-donating, *para*-methoxy substituent. This outcome is consistent with the reported oxidation potential of **166d** (E_{ox} = +0.26 V vs. SCE) [68] and related electron-rich species, whose conversion to carbocations by Ir(IV) (E_{ox} = +0.77 V vs. SCE) [38] is energetically feasible. Finally, a Mukaiyama-type, polar, and vinylogous benzylation between **135a** and **167d** takes place, affording the corresponding γ-benzyl butenolide **164ad**. To showcase the practical value of the photoinduced benzylation protocols and the versatility of the resulting benzylbutenolide frameworks, the authors further applied both methodologies to synthesize a series of bioactive, chiral hydroxyphenyl-γ-valerolactones, as well as a racemic 4-(hydroxyphenyl)valeric acid derivative (not shown).

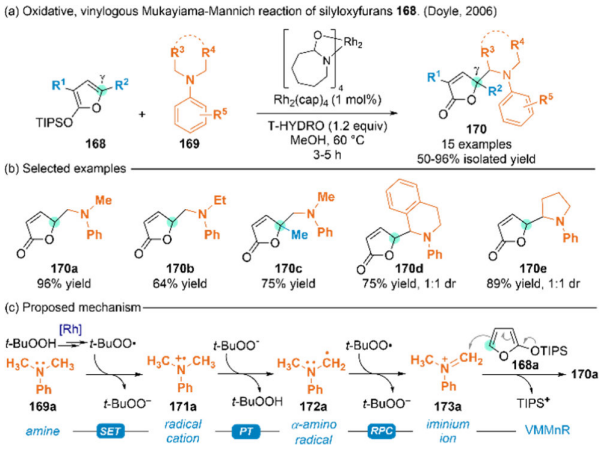
Another noble example of an RPC pathway applied to a polar transformation is the oxidative Mukaiyama–Mannich reaction (oxidative MMnR), which represents an attractive alternative to the classical indirect polar approaches, wherein a silyl enol ether or silyl ketene acetal adds to a (pre)formed imine or iminium ion by way of a suitable catalyst, to generate the corresponding β-aminocarbonyl adduct. The oxidative variant relies instead on the direct C—H oxidation of a tertiary amine **IX** to generate the corresponding iminium ion **XI** via a radical-mediated RPC mechanism (Scheme 30) [69]. According to the most widely accepted mechanism, an initial single-electron oxidation of **IX** generates the corresponding radical cation **X**, which can follow two distinct pathways: (i), it may undergo hydrogen atom transfer (HAT) to form the corresponding iminium ion **XI**; or (ii), in the presence of a base, it may be deprotonated at the α-position to afford the α-amino radical **XII**, which can subsequently be oxidized by a second single-electron event to yield **XI**. Historically, these reactions were promoted using stoichiometric oxidants. In recent years, however, photoredox and electrochemical oxidation strategies have emerged, significantly expanding the scope and versatility of the overall process [69].

Although the oxidative MMnR of silyl enol ethers and silyl ketene acetals is a well-established transformation, the corresponding vinylogous variant, namely the oxidative, vinylogous Mukaiyama–Mannich reaction (oxidative VMMnR), has remained comparatively underexplored since the pioneering work by Doyle and coworkers in 2006 [70].

The Doyle's group developed a mild, selective, and efficient transition metal-catalyzed oxidative VMMnR between silyloxyfurans **168** and a variety of *N*, *N*-dialkylanilines **169**. The transformation was promoted by catalytic dirhodium caprolactamate [Rh_2(cap)$_4$] under an aerobic atmosphere, using *tert*-butyl hydroperoxide



SCHEME 30 | The oxidative Mukaiyama–Mannich reaction by way of a RPC strategy to generate iminium ion **XI** through C—H oxidation of a tertiary amine **IX**.



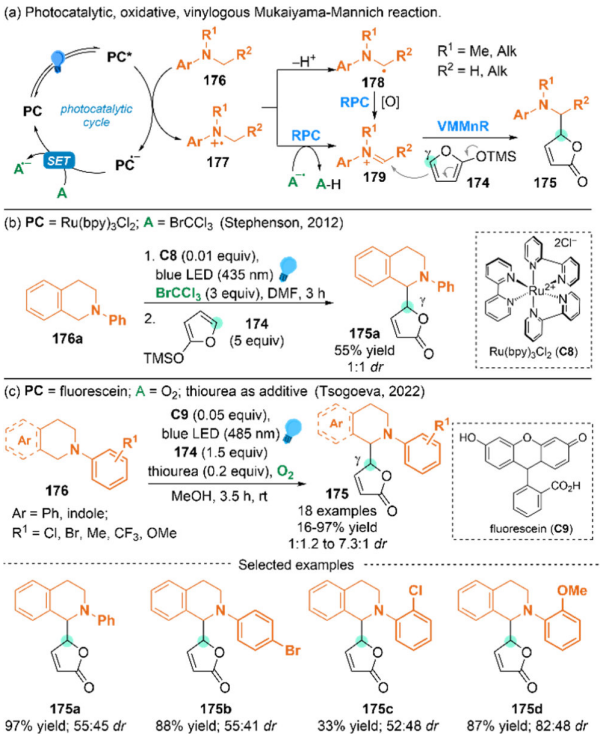
SCHEME 31 | The first, oxidative, vinylogous Mukaiyama–Mannich reaction developed by Doyle et al. Yields refer to NMR yields. Relative configurations not determined. SET = single-electron transfer; PT = proton transfer; RPC = radical–polar crossover; VMMnR = vinylogous Mukaiyama–Mannich reaction.

(TBHP or T-HYDRO, 70% in water) as the stoichiometric oxidant (Scheme 31a). Conducted in MeOH at 60 °C for several hours, the reaction furnished a set of fifteen γ-aminoalkyl butenolides **170** in good-to-excellent isolated yields (50%–95%) with complete γ-regioselectivity. The method showed broad scope, accommodating a wide array of anilines bearing diverse substituents on both the aromatic ring and the alkyl chains. Notably, high site selectivity was observed for unsymmetrical anilines containing both *N*-methyl and *N*-methylene groups, with functionalization occurring preferentially at the less hindered methyl substituent (e.g., compounds **170aa–170ae**, Scheme 31b). Furthermore, 2-methyl-, 4-methyl, and 4-allyl-substituted silyloxyfurans proved also viable substrates, all adding the imine at the γ-position with good yields (e.g., adduct **170ac**, Scheme 31b). A comprehensive mechanistic investigation of the Rh_2(cap)$_4$-catalyzed oxidative Mannich reaction with TBHP was assessed by Doyle several years later [71]. After in-depth analysis of the reaction by way of linear free-energy relationship, kinetic and product isotope effects, radical trap experiments, as well as kinetic studies of the oxidative Mannich reaction in different solvents, the authors ended up with a solid proposal based on an oxidative RPC mechanism. As shown in Scheme 31c with *N*, *N*-dimethylaniline **169a** as a representative example, the proposed mechanism starts with a rate-determining single-electron oxidation (SET) of **169a** to the corresponding radical cation **171a** by *tert*-butylperoxy radical initially generated from TBHP with Rh_2(cap)$_4$. This is followed by an irreversible heterolytic cleavage of the C—H bond at the α-position to nitrogen to give the corresponding α-amino radical **172a**. Thus, a second molecule of *tert*-butylperoxy radical promotes the oxidation of the radical intermediate to the corresponding iminium ion **173a** the RPC event that is subsequently trapped by the silyloxyfuran **168a** to generate the final product **170aa**. Interestingly, an alternative pathway involving molecular oxygen as the oxidant (not shown) was also considered, although it proved to be more suitable for related transformations promoted by other transition-metal complexes (e.g., copper, iron, and cobalt). Regarding the site selectivity observed in the vinylogous addition of **168a** to the methyl group of unsymmetrical anilines, the authors propose that this preference arises from both acidity and steric effects of the alkyl chains linked to the nitrogen. Another option to promote

10990690, 0, Downloaded from https://chemistry-europe.onlinelibrary.wiley.com/doi/10.1002/ejoc.70753 by Claudio Curti - University Degli Studi Di Parma Stampa Universitaria Parmense , Wiley Online Library on [31/08/2026]. See the Terms and Conditions (https://onlinelibrary.wiley.com/terms-and-conditions) on Wiley Online Library for rules of use; OA articles are governed by the applicable Creative Commons License

the oxidative VMMnR starting from a tertiary amine is the use of visible-light photoredox catalysis. As shown in Scheme 32a, the combination of visible light with a suitable photocatalyst **PC** and a stoichiometric oxidant **A** under mild conditions enables the photocatalytic oxidation of a tertiary amine **176** to the corresponding iminium ion **179**, via the formation of the amine radical cation intermediate **177**. The use of amines as reductants for photocatalysis is ideal, because trialkyl amines are inexpensive, ubiquitous, and readily oxidized [72].

In this context, Stephenson and coworkers first demonstrated the feasibility of this strategy in 2012 by reporting, within a broader investigation, a single example of an oxidative VMMnR promoted by visible-light photoredox catalysis, between trimethylsilyloxyfuran **174** and *N*-phenyl tetrahydroisoquinoline **176a** (Scheme 32b) [73]. Using $Ru(bpy)_3Cl_2$ (**C8**, 1 mol%) as the photocatalyst and $BrCCl_3$ as the stoichiometric oxidant under blue-light irradiation (435 nm) and mild conditions (DMF, room temperature, 3 h), the authors obtained the sole γ-alkylated butenolide **175a** regioselectively at the α-benzylic position of **176a** in a 55% isolated yield as a 1:1 mixture of *syn/anti*-isomers. The authors proposed a mechanism based on a photocatalytic cycle, albeit without ruling out a radical chain alternative. Concerning the former proposal and following the general pathway of Scheme 32a, the excited Ru^{2+}* first oxidizes the *N*-aryltetrahydroisoquinoline **176a** to the corresponding radical cation **177a** (not shown). The resulting Ru^{+}, in turn, closes the cycle by reducing $BrCCl_3$ to Br^- and the trichloromethyl radical ($Cl_3C\bullet$). The oxidative RPC is then secured by a regioselective H-atom abstraction (HAT) by the trichloromethyl radical onto the benzyl carbon of **177a**, hence affording the reactive iminium ion **179a** susceptible to the polar, vinylogous trapping by **174**. More recently, in 2022, similar tetrahydroisoquinoline congeners **175** were accessed by Alabugin, Tsogoeva, and coworkers with an alternative oxidative VMMnR based on a metal-free, visible light-driven one pot/two-step procedure (Scheme 32c) [74]. The combination of fluorescein (**C9**) as photosensitizer (5 mol%) and thiourea as a substoichiometric (0.2 mol equiv) additive in the presence of molecular oxygen was found to be the most effective way to promote the oxidative VMMnR between a series of *N*-aryl tetrahydroisoquinolines **176** and trimethylsilyloxyfuran **174** to afford various γ-alkylbutenolides **175** in low-to-excellent yields (16%–97%) and different diastereomeric ratios (d.r.) spanning from 1:1.2 to 7.3:1 (relative configuration not determined). A correlation between the yield of the reaction and the substitution pattern within the aryl substituent at the nitrogen of **176** was observed. Electron-withdrawing groups (EWG) (e.g., chlorine and bromine) or weakly electron-donating groups (EDG) like the methyl group gave higher yields of the products when in *para*- or *meta*-position, but lower yields when in the *ortho*-position (compare compounds **175b** and **175c** in Scheme 32c). Stronger EDGs like the methoxy group had a better effect when in the *ortho*-position (see compound **175b**). Also, the reaction proved viable on indole-fused pyrrolidines (triptoines), although in lower yields (not shown). Both experimental and computational data supported a photocatalytic pathway in which the key amine radical cation is formed through single-electron oxidation (SET) of tertiary amine **176**, promoted by photoexcited fluorescein under blue-light irradiation (485 nm). Catalyst turnover then occurs via electron transfer between ambient molecular oxygen and the reduced fluorescein, generating the superoxide radical anion ($O_2^{\bullet-}$). This reactive species can follow two possible routes. It may deprotonate the amine radical cation **177**, producing the corresponding α-amino radical **178**, which is then oxidized to form iminium ion **179**. Alternatively and consistent with the previously described mechanism, $O_2^{\bullet-}$ can directly abstract a hydrogen atom from **177** in a homolytic fashion, giving iminium ion **179** in a single step. Interestingly, data also indicate that thiourea plays a crucial role in the success of the reaction, likely due to its ability to act as an electron-transfer mediator and/or to scavenge reactive oxygen species. Finally, the resulting tetrahydroisoquinoline-butenolide hybrid compounds **175** exhibited strong in vitro antischistosomal and anticancer activities.



SCHEME 32 | Photocatalytic, oxidative, vinylogous Mukaiyama–Mannich reaction. (a) General mechanism. (b) Seminal contribution by Stephenson in 2012. (c) Metal-free variant introduced by Tsogoeva in 2022. RPC = radical–polar crossover. SET = single-electron transfer.

5 | Summary and Outlook

In summary, π-extended silyl polyenol ethers and their related silyl ketene acetals have emerged as highly versatile platforms in radical chemistry, complementing their well-established role as vinylogous nucleophiles in polar transformations. As extensively discussed, their intrinsically electron-rich nature, arising from the conjugated π-system and the σ-donating effect of the silyl group, underpins both their classical reactivity and their growing relevance in single-electron processes. Within this framework, these systems display remarkable versatility, acting as electron-rich SOMOphiles, radical precursors, and nucleophilic partners in RPC processes. When operating as SOMOphiles, their pronounced tendency toward remote functionalization (γ-, ε-, η-positions) represents a hallmark of their radical chemistry and arises from a subtle interplay of electronic delocalization, steric effects, and radical stabilization across the extended π-system.

10990690, 0, Downloaded from https://chemistry-europe.onlinelibrary.wiley.com/doi/10.1002/ejoc.70753 by Claudio Curti - University Degli Studi Di Parma Stampa Universitaria Parmense , Wiley Online Library on [31/08/2026]. See the Terms and Conditions (https://onlinelibrary.wiley.com/terms-and-conditions) on Wiley Online Library for rules of use; OA articles are governed by the applicable Creative Commons License

A key conceptual feature that distinguishes these substrates in radical manifolds is their ability to undergo umpolung reactivity upon single-electron oxidation. While in polar reactions they behave as nucleophilic vinylogous enolates (HOMO-controlled reactivity), oxidation enables their conversion into silyl radical cations or the corresponding keto-allyl radicals, which display electrophilic character (SOMO-controlled reactivity). This polarity inversion significantly broadens their reactivity profile, allowing access to unconventional bond-forming processes that are typically inaccessible through traditional two-electron pathways. Also, recent advances driven by photoredox catalysis and electrochemistry have further expanded the synthetic utility of these systems. These approaches have enabled efficient C—C and C—heteroatom bond formation, the development of enantioselective variants, and applications in the synthesis of complex molecules and natural products. Despite these achievements, several challenges and opportunities remain. A deeper understanding of the factors governing regio- and stereocontrol in these vinylogous radical processes—especially in the presence of multiple reactive sites and open-shell intermediates—is still required. Moreover, the development of more general enantioselective protocols, as well as sustainable and scalable catalytic systems, particularly those based on visible light and electrochemistry, will be essential to fully unlock their potential. Finally, by leveraging the switchable polarity of these systems, future methodologies may exploit their dual reactivity in a programmable fashion, enabling increasingly efficient and selective synthetic strategies. Overall, the growing body of work discussed in this review clearly positions π-extended silyl polyenol ethers as privileged scaffolds in modern synthetic chemistry, and continued research in this rapidly evolving area will further consolidate their role as key enabling tools for molecular construction.

Acknowledgments

This work was carried out in the frame of the ALIFAR project within the program "Dipartimenti di Eccellenza 2023-2027" of the Italian Ministry of University.

Open access publishing facilitated by Universita degli Studi di Parma, as part of the Wiley - CRUI-CARE agreement.

Funding

The author has nothing to report.

Conflicts of Interest

The authors declare no conflicts of interest.

Data Availability Statement

The data that support the findings of this study are available from the corresponding author upon reasonable request.

References

1. C. Curti, L. Battistini, A. Sartori, and F. Zanardi, "New Developments of the Principle of Vinylogy as Applied to π-Extended Enolate-Type Donor Systems," *Chemical Review* 120 (2020): 2448–2612.

2. R. C. Fuson, "The Principle of Vinylogy," *Chemical Review* 16 (1935): 1–27.

3. M. Cordes and M. Kalesse, "Very Recent Advances in Vinylogous Mukaiyama Aldol Reactions and Their Applications to Synthesis," *Molecules* 24 (2019): 3040.

4. S. F. Martin, "Evolution of the Vinylogous Mannich Reaction as a Key Construction for Alkaloid Synthesis," *Accounts of Chemical Research* 35 (2002): 895–904.

5. Y. Yin and Z. Jiang, "Organocatalytic Asymmetric Vinylogous Michael Reactions," *ChemCatChem* 9 (2017): 4306–4318.

6. J. Wang, C. Guo, Y. Liu, Y. Ji, H. Jia, and H. Li, "Enantioselective Synthesis of the 1,3-Dienyl-5-Alkyl-6-Oxy Motif: Method Development and Total Synthesis," *Angewandte Chemie International Edition* 63 (2024): e202400478.

7. S. Jemail, E. Magnier, M. R. Vitale, and G. Dagousset, "Advances in Radical Remote γ-Functionalization of α,β-Unsaturated Carbonyl Compounds," *Synthesis* 58 (2025): 1–16.

8. Y. Zhang, Y. Zhang, and C. Li, "Radical Retrosynthesis: A Powerful Strategy for Modern Assembly of Terpenoid Natural Products," *Chemical Society Reviews* 54 (2025): 10427–10486.

9. J. Li, D. Zhang, Z. Hu, and Z. Yuan, "Illuminating the Transformation of Photocatalysts in Light-Driven Organic Synthesis," *Nature Catalysis* 8 (2025): 1268–1280.

10. S. Möhle, M. Zirbes, E. Rodrigo, T. Gieshoff, A. Wiebe, and S. R. Waldvogel, "Modern Electrochemical Aspects for the Synthesis of Value-Added Organic Products," *Angewandte Chemie International Edition* 57 (2018): 6018–6041.

11. H.-M. Huang, M. H. Garduño-Castro, C. Morrill, and D. J. Procter, "Catalytic Cascade Reactions by Radical Relay," *Chemical Society Reviews* 48 (2019): 4626–4638.

12. B. Giese, "Formation of CC Bonds by Addition of Free Radicals to Alkenes," *Angewandte Chemie International Edition* 22 (1983): 753–764.

13. J. D. Bell and J. A. Murphy, "Recent Advances in Visible Light-Activated Radical Coupling Reactions Triggered by (i) Ruthenium, (ii) Iridium and (iii) Organic Photoredox Agents," *Chemical Society Reviews* 50 (2021): 9540–9685.

14. F. Parsaee, M. C. Senarathna, P. B. Kannangara, S. N. Alexander, P. D. E. Arche, and E. R. Welin, "Radical Philicity and Its Role in Selective Organic Transformations," *Nature Reviews Chemistry* 5 (2021): 486–499.

15. K. Héberger and A. Lopata, "Assessment of Nucleophilicity and Electrophilicity of Radicals, and of Polar and Enthalpy Effects on Radical Addition Reactions," *Journal of Organic Chemistry* 63 (1998): 8646–8653.

16. F. De Vleeschouwer, V. Van Speybroeck, M. Waroquier, P. Geerlings, and F. De Proft, "Electrophilicity and Nucleophilicity Index for Radicals," *Organic Letters* 9 (2007): 2721–2724.

17. F. D. Vleeschouwer, V. V. Speybroeck, M. Waroquier, P. Geerlings, and F. D. Proft, "An Intrinsic Radical Stability Scale From the Perspective of Bond Dissociation Enthalpies: A Companion to Radical Electrophilicities," *Journal of Organic Chemistry* 73 (2008): 9109–9120.

18. M. Spichty, H. Zipse, S. Majouri, K. M. Fromm, and B. Giese, "50 Years of Giese Reaction – a Personal View," *Angewandte Chemie International Edition* 65 (2026): e24825.

19. C. C. Nawrat, C. R. Jamison, Y. Slutskyy, D. W. C. MacMillan, and L. E. Overman, "Oxalates as Activating Groups for Alcohols in Visible Light Photoredox Catalysis: Formation of Quaternary Centers by Redox-Neutral Fragment Coupling," *Journal of the American Chemical Society* 137 (2015): 11270–11273.

20. P. V. Pham, D. A. Nagib, and D. W. C. MacMillan, "Photoredox Catalysis: A Mild, Operationally Simple Approach to the Synthesis

10990690, 0, Downloaded from https://chemistry-europe.onlinelibrary.wiley.com/doi/10.1002/ejoc.70753 by Claudio Curti - University Degli Studi Di Parma Stampa Universitaria Parmense , Wiley Online Library on [31/08/2026]. See the Terms and Conditions (https://onlinelibrary.wiley.com/terms-and-conditions) on Wiley Online Library for rules of use; OA articles are governed by the applicable Creative Commons License

of α-Trifluoromethyl Carbonyl Compounds," *Angewandte Chemie International Edition* 50 (2011): 6119–6122.

21. W. Kong, C. Yu, H. An, and Q. Song, "Photoredox-Catalyzed Decarboxylative Alkylation of Silyl Enol Ethers to Synthesize Functionalized Aryl Alkyl Ketones," *Organic Letters* 20 (2018): 349–352.

22. S. E. Denmark, J. R. Heemstra Jr., and G. L. Beutner, "Catalytic, Enantioselective, Vinylogous Aldol Reactions," *Angewandte Chemie International Edition* 44 (2005): 4682–4698.

23. G. Casiraghi, L. Battistini, C. Curti, G. Rassu, and F. Zanardi, "The Vinylogous Aldol and Related Addition Reactions: Ten Years of Progress," *Chemical Reviews* 111 (2011): 3076–3154.

24. J. Zhang, M. Liu, W. Zhang, and C. Guo, "Enantioselective Electrochemical Nickel-Catalyzed Vinylogous Radical Reactions," *Science Advances* 11 (2025): eadu5594.

25. R. Pucci and G. G. N. Angilella, "Density Functional Theory, Chemical Reactivity, and the Fukui Functions," *Foundations of Chemistry* 24 (2022): 59–71.

26. P. Morgante and J. Autschbach, "Strategies to Calculate Fukui Functions and Applications to Radicals With SOMO–HOMO Inversion," *Journal of Chemical Theory and Computation* 19 (2023): 3929–3942.

27. V. Nair, T. G. George, A. Augustine, and L. G. Nair, "Cerium(IV) Ammonium Nitrate Mediated Thiocyanation of Dienes: Some Interesting Observations," *Research on Chemical Intermediates* 26 (2000): 923–929.

28. In the original report, product 14 was depicted with a cis configuration, although no experimental or spectroscopic evidence supporting this assignment was discussed. In light of this, it is plausible that the actual product formed may instead possess a trans configuration.

29. S. Kim and C. J. Lim, "Radical-Mediated γ-Functionalizations of α,β-Unsaturated Carboxylic Amides," *Angewandte Chemie International Edition* 43 (2004): 5378–5380.

30. S. Kim, C. J. Lim, C. Song, and W. Chung, "Novel Radical Alkylation of Carboxylic Imides," *Journal of the American Chemical Society* 124 (2002): 14306–14307.

31. J. Y. Lee and S. Kim, "Tin-Free, Radical-Mediated γ-Alkylations of α,β-Unsaturated Esters via O-Tert-Alkyl Dienol Ethers," *Synlett* 2008 (2008): 49–54.

32. X. Liu, X. Chen, and J. T. Mohr, "Copper-Catalyzed γ-Sulfonylation of α,β-Unsaturated Carbonyl Compounds by Means of Silyl Dienol Ethers," *Organic Letters* 17 (2015): 3572–3575.

33. X. Chen, X. Liu, and J. T. Mohr, "Cu-Catalyzed Stereoselective γ-Alkylation of Enones," *Journal of the American Chemical Society* 138 (2016): 6364–6367.

34. X.-X. Guo, D.-W. Gu, Z. Wu, and W. Zhang, "Copper-Catalyzed C–H Functionalization Reactions: Efficient Synthesis of Heterocycles," *Chemical Reviews* 115 (2015): 1622–1651.

35. X. Liu, X. Chen, and J. T. Mohr, "Cascade Mn-Mediated γ-Alkylation/Oxa-Michael Addition of Enones With 1,3-Dicarbonyls," *Chemistry – a European Journal* 22 (2016): 2274–2277.

36. X. Liu, X. Chen, and J. T. Mohr, "Regiocontrolled Oxidative C–C Coupling of Dienol Ethers and 1,3-Dicarbonyl Compounds," *Organic Letters* 18 (2016): 3182–3185.

37. D. C. Yarbrough, B. K. Osei-Badu, C. J. Wagner, K. R. Storme, R. S.J.Marquez, and J. T. Mohr, "Fe-Catalyzed Structurally Divergent γ-Polyhaloalkylation of Siloxydienes," *Organic Letters* 26 (2024): 10735–10739.

38. C. K. Prier, D. A. Rankic, and D. W. C. MacMillan, "Visible Light Photoredox Catalysis With Transition Metal Complexes: Applications in Organic Synthesis," *Chemical Reviews* 113 (2013): 5322–5363.

39. K. F. Szabó, K. Goliszewska, J. Szurmak, K. Rybicka-Jasińska, and D. Gryko, "Site-Selective, Photocatalytic Vinylogous Amidation of Enones," *Organic Letters* 24 (2022): 8120–8124.

40. M. Briand, L. D. Thai, F. Bourdreux, et al., "Remote Radical Trifluoromethylation: A Unified Approach to the Selective Synthesis of γ-Trifluoromethyl α,β-Unsaturated Carbonyl Compounds," *Organic Letters* 24 (2022): 9375–9380.

41. C. Banoun, F. Bourdreux, and G. Dagousset, "Highly Selective γ-Alkoxylation, γ-Amination and γ-Alkylation of Unbiased Enals by Means of Photoredox Catalysis," *Chemical Communications* 59 (2023): 760–763.

42. M. Briand, E. Magnier, E. Anselmi, and G. Dagousset, "Photocatalyzed One-Pot Selective Synthesis of γ-(per)fluoroalkenylated α,β-Unsaturated Carbonyl Compounds," *Advanced Synthesis & Catalysis* 366 (2024): 3494–3499.

43. F. Ye, S. Zhang, Z. Wei, et al., "Versatile Fluorinated Building Blocks by Stereoselective (per)fluoroalkenylation of Ketones," *European Journal of Organic Chemistry* 2020 (2020): 70–81.

44. C. Banoun, F. Bourdreux, E. Magnier, and G. Dagousset, "Site-Selective γ-Trihalomethylation and γ-Dihalomethylidenation of Silyl Dienol Ethers Under Organophotoredox Catalysis," *Chemistry – a European Journal* 31 (2025): e202403598.

45. D. Spinnato, B. Schweitzer-Chaput, G. Goti, M. Ošeka, and P. Melchiorre, "A Photochemical Organocatalytic Strategy for the α-Alkylation of Ketones by Using Radicals," *Angewandte Chemie International Edition* 59 (2020): 9485–9490.

46. X. Tan, Z. Song, X. Liang, et al., "Regioselective Syntheses of 1,4- and 1,6-Dicarbonyl Compounds via Photoredox-Based Oxidative Heterocoupling of Enolsilanes With Oxygen as an Oxidant," *Organic Letters* 26 (2024): 5403–5408.

47. D. Guazzetti, L. Aimi, E. Marcantonio, et al., "Photoinduced, Chemoselective γ-Alkylation of 2-Silyloxyfurans With α-Bromoketones: A Rapid Entry to Chiral ε-Keto-γ-Butenolides," *Chemistry – a European Journal* 32 (2026): e03083.

48. N. Li, X. Ye, Y. Liu, and J. Song, "Enantioselective Radical α-Enolation of Esters via Electrochemical Chiral Isothiourea Catalysis," *Nature Catalysis* 8 (2025): 957–967.

49. L. You, X. T. Liang, L. M. Xu, et al., "Asymmetric Total Synthesis of Propindilactone G," *Journal of the American Chemical Society* 137 (2015): 10120–10123.

50. B. K. Osei-Badu and J. T. Mohr, "Total Synthesis of Panaxydiol and (−)-Virol C," *Journal of Organic Chemistry* 90 (2025): 15117–15121.

51. G. Yue and B. Liu, "The Photoinduced Electron Transfer (PET) Reactions of Silyl Ethers and Their Application," *Tetrahedron Chemistry* 9 (2024): 100067.

52. D. Seebach, "Methods of Reactivity Umpolung," *Angewandte Chemie International Edition* 18 (1979): 239–258.

53. P. G. Gassman and K. J. Bottorff, "Electron Transfer Induced Desilylation of Trimethylsilyl Enol Ethers," *Journal of Organic Chemistry* 53 (1988): 1097–1100.

54. B. B. Snider and T. Kwon, "Oxidative Cyclization of .σ,ε- and ε,ζ-Unsaturated Enol Silyl Ethers and Unsaturated Siloxycyclopropanes," *Journal of Organic Chemistry* 57 (1992): 2399–2410.

55. S. Fukuzumi, M. Fujita, J. Otera, and Y. Fujita, "Electron-Transfer Oxidation of Ketene Silyl Acetals and Other Organosilanes. Mechanistic Insight Into Lewis Acid Mediated Electron Transfer," *Journal of the American Chemical Society* 114 (1992): 10271–10278.

56. D. Rehm and A. Weller, "Kinetics of Fluorescence Quenching by Electron and H-Atom Transfer," *Israel Journal of Chemistry* 8 (1970): 259–271.

57. M. Schmittel, M. Kelley, and A. Burghart, "Silyl Enol Ether Cation Radicals in Solution: Nucleophile Assisted Si–O Bond Cleavage," *Journal of the Chemical Society, Perkin Transactions 2* 24 (1995): 2327–2333.

10990690, 0, Downloaded from https://chemistry-europe.onlinelibrary.wiley.com/doi/10.1002/ejoc.70753 by Claudio Curti - University Degli Studi Di Parma Stampa Universitaria Parmense , Wiley Online Library on [31/08/2026]. See the Terms and Conditions (https://onlinelibrary.wiley.com/terms-and-conditions) on Wiley Online Library for rules of use; OA articles are governed by the applicable Creative Commons License

58. E. Marcantonio, D. Guazzetti, L. Aimi, et al., "Harnessing Vinylogy With Radicals: Photoinduced γ-Benzylation Reactions of 2-Silyloxyfurans," *Advanced Synthesis & Catalysis* 367 (2025): e70035.

59. A. B. Paolobelli, D. Latini, and R. Ruzziconi, "γ-Selectivity in the Ceric Ammonium Nitrate Promoted Oxidative Addition of Silyl Dienol Ethers to Silyl Enol Ethers," *Tetrahedron Letters* 34 (1993): 721–724.

60. P. Langer and V. Köhler, "First Oxidative Cyclization of 1,3-Bis(trimethylsilyloxy)buta-1,3-Dienes," *Chemical Communications* 17 (2000): 1653–1654.

61. M. Mitani, H. Sakata, and H. Tabei, "Addition Reactions of Polyhalides to Ketene Silyl Acetals and Silyl Enol Ethers Under Thermal or Photo-Irradiated Conditions Without a Promoter," *Bulletin of the Chemical Society of Japan* 75 (2002): 1807–1814.

62. D. Galaktionova, X. Liu, X. Chen, and J. T. Mohr, "Iron-Catalyzed Gamma-Gamma Dimerization of Siloxydienes," *Chemistry – A European Journal* 30 (2024): e202302901.

63. P. Mena, L. Bresciani, N. Brindani, et al., "Phenyl-γ-Valerolactones and Phenylvaleric Acids, the Main Colonic Metabolites of Flavan-3-Ols: Synthesis, Analysis, Bioavailability, and Bioactivity," *Natural Product Reports* 36 (2019): 714–752.

64. R. J. Wiles and G. A. Molander, "Photoredox-Mediated Net-Neutral Radical/Polar Crossover Reactions," *Israel Journal of Chemistry* 60 (2020): 281–293.

65. Z. Zhu, Y. Zhang, Z. Li, and C. Shu, "Photoinduced Radical-Polar Crossover Cyclization Reactions," *Chem Catalysis* 4 (2024): 100945.

66. X. Guo, K. Wu, and M. Zhang, "Recent Progress in Asymmetric Oxidative Radical–Polar Crossover Reactions," *Advanced Synthesis & Catalysis* 368 (2026): e70315.

67. L. Pitzer, J. L. Schwarz, and F. Glorius, "Reductive Radical-Polar Crossover: Traditional Electrophiles in Modern Radical Reactions," *Chemical Science* 10 (2019): 8285–8291.

68. K. Ishiguro, T. Nakano, H. Shibata, and Y. Sawaki, "Redox Reaction of Benzyl Radicals With Aromatic Radical Ions Photogenerated. The Marcus Inverted Region and the Selective Formation of Carbocations or Carbanions," *Journal of the American Chemical Society* 118 (1996): 7255–7264.

69. C.-J. Long, Y.-H. He, and Z. Guan, "Asymmetric Oxidative Mannich Reactions Promoted by Photocatalysis and Electrochemistry," *Organic & Biomolecular Chemistry* 20 (2022): 2544–2561.

70. A. J. Catino, J. M. Nichols, B. J. Nettles, and M. P. Doyle, "The Oxidative Mannich Reaction Catalyzed by Dirhodium Caprolactamate," *Journal of the American Chemical Society* 128 (2006): 5648–5649.

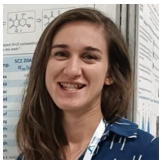
71. M. O. Ratnikov and M. P. Doyle, "Mechanistic Investigation of Oxidative Mannich Reaction With Tert -Butyl Hydroperoxide. The Role of Transition Metal Salt," *Journal of the American Chemical Society* 135 (2013): 1549–1557.

72. J. Hu, J. Wang, T. H. Nguyen, and N. Zheng, "The Chemistry of Amine Radical Cations Produced by Visible Light Photoredox Catalysis," *Beilstein Journal of Organic Chemistry* 9 (2013): 1977–2001.

73. D. B. Freeman, L. Furst, A. G. Condie, and C. R. J. Stephenson, "Functionally Diverse Nucleophilic Trapping of Iminium Intermediates Generated Utilizing Visible Light," *Organic Letters* 14 (2012): 94–97.

74. L. Kersting, L. Kuhn, M. Anokhin, et al., "Visible-Light-Driven Metal-Free C–H Functionalization: Access to New Bioactive Tetrahydroisoquinoline-Butenolide Hybrids via Domino Amine Oxidation/Vinylogous Mannich Reaction," *ChemPhotoChem* 6 (2022): e202200109.

Biographies



Debora Guazzetti graduated in Pharmaceutical Chemistry and Technology in 2022 at the University of Parma, where she also earned her Ph.D. in 2026. Her doctoral research focused on the development of synthetic methodologies for accessing bioactive heterocyclic scaffolds through the integration of organocatalysis and photocatalysis. She is currently a postdoctoral researcher at the Max Planck Institute for Chemical Energy Conversion (Mülheim an der Ruhr) in the group of Prof. S. R. Waldvogel, where she works on organic electrosynthesis.



Kelly Bugatti is a Tenure-Track Researcher in Organic Chemistry at the University of Parma, Italy (Food and Drug Department). She earned a degree in Chemistry and Pharmaceutical Technology in 2017 and a Ph.D. in 2021 at the same university. Her research focuses on the synthesis of heterocycles, peptide synthesis, and characterization, linking drug development and food science. She studies conjugated peptides for targeting and imaging tumors and fibrosis, and analyzes epitopes from novel foods with allergenic potential while synthesizing molecules that interact with taste receptors.



Claudio Curti is an Associate Professor in Organic Chemistry at the University of Parma (Italy), where he works in the Department of Food and Drug. He graduated in Pharmaceutical Chemistry and Technology in 2002 and completed advanced studies at the School of Chemical Synthesis, University of Milan, in 2005. His research focuses on asymmetric, vinylogous, and hypervinylogous processes integrated with organocatalysis and photocatalysis, aimed at the efficient synthesis of bioactive compounds.



Franca Zanardi is a Professor in Organic Chemistry at the University of Parma, where she earned her Ph.D. in Bio-Organic Chemistry in 1996. Her research interests include the application of the vinylogy concept in the selective (asymmetric) synthesis of medicinally/food-relevant heterocycles, as well as the use of peptidomimetic chemistry applied to cancer- and inflammation-related diseases. She is recipient of the "Adolfo Quilico" Medal 2024 from the Organic Chemistry Division of the Italian Chemical Society.

10990690, 0, Downloaded from https://chemistry-europe.onlinelibrary.wiley.com/doi/10.1002/ejoc.70753 by Claudio Curti - University Degli Studi Di Parma Stampa Universitaria Parmense , Wiley Online Library on [31/08/2026]. See the Terms and Conditions (https://onlinelibrary.wiley.com/terms-and-conditions) on Wiley Online Library for rules of use; OA articles are governed by the applicable Creative Commons License